(12) INTERNATIONAL APPLICATION PUBLISHED UNDER THE PATENT COOPERATION TREATY (PCT)

(19) World Intellectual Property Organization
International Bureau

(43) International Publication Date
27 October 2016 (27.10.2016)

WIPO | PCT

(10) International Publication Number
WO 2016/172498 A1

(51) International Patent Classification:
A61P 31/06 (2006.01) *A61K 31/505* (2006.01)
A61K 31/4164 (2006.01)

(21) International Application Number:
PCT/US2016/028867

(22) International Filing Date:
22 April 2016 (22.04.2016)

(25) Filing Language: English

(26) Publication Language: English

(30) Priority Data:
62/151,220 22 April 2015 (22.04.2015) US

(71) Applicant: **THE TEXAS A&M UNIVERSITY SYSTEM** [US/US]; 3369 TAMU, College Station, TX 77843-3369 (US).

(72) Inventors: **SACCHETTINI, James, C.**; 5720 Blue Ridge Drive, College Station, TX 77845 (US). **AGGARWAL, Anup**; 800 Marion Pugh Drive, #812, College Station, TX 77840 (US). **PARAI, Maloy, K.**; 1301 Barthelow Drive, #8B, College Station, TX 77840 (US).

(74) Agent: **LECOINTE, Michelle**; Baker Botts L.L.P., 2001 Ross Avenue, Suite 600, Dallas, TX 75201 (US).

(81) Designated States *(unless otherwise indicated, for every kind of national protection available)*: AE, AG, AL, AM, AO, AT, AU, AZ, BA, BB, BG, BH, BN, BR, BW, BY, BZ, CA, CH, CL, CN, CO, CR, CU, CZ, DE, DK, DM, DO, DZ, EC, EE, EG, ES, FI, GB, GD, GE, GH, GM, GT, HN, HR, HU, ID, IL, IN, IR, IS, JP, KE, KG, KN, KP, KR, KZ, LA, LC, LK, LR, LS, LU, LY, MA, MD, ME, MG, MK, MN, MW, MX, MY, MZ, NA, NG, NI, NO, NZ, OM, PA, PE, PG, PH, PL, PT, QA, RO, RS, RU, RW, SA, SC, SD, SE, SG, SK, SL, SM, ST, SV, SY, TH, TJ, TM, TN, TR, TT, TZ, UA, UG, US, UZ, VC, VN, ZA, ZM, ZW.

(84) Designated States *(unless otherwise indicated, for every kind of regional protection available)*: ARIPO (BW, GH, GM, KE, LR, LS, MW, MZ, NA, RW, SD, SL, ST, SZ, TZ, UG, ZM, ZW), Eurasian (AM, AZ, BY, KG, KZ, RU,

[Continued on next page]

(54) Title: SUBSTITUTED BENZOFURAN DERIVATIVES AS NOVEL ANTIMYCOBACTERIAL AGENTS

(57) Abstract: Novel bacterial inhibitors comprising benzofuran derivatives, and methods of bacterial inhibition using the inhibitors are disclosed. The inhibitors may inhibit, for example, mycobacteria, including *M. tuberculosis*, by inhibition of the Pksl3 enzyme. The inhibitors cmat exhibit potent whole cell and *in vivo* efficacy against *M. tuberculosis*.

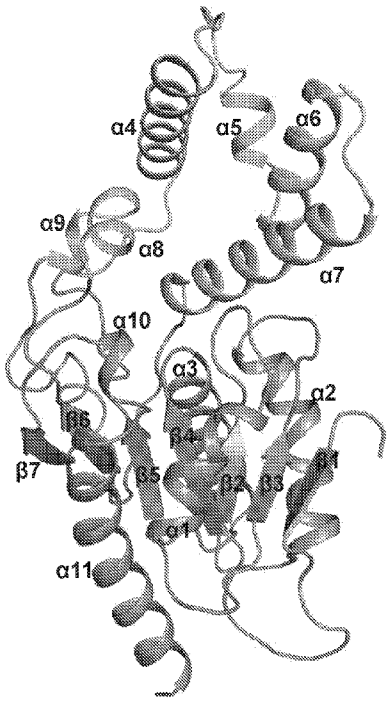

FIG. 1

WO 2016/172498 A1

TJ, TM), European (AL, AT, BE, BG, CH, CY, CZ, DE, DK, EE, ES, FI, FR, GB, GR, HR, HU, IE, IS, IT, LT, LU, LV, MC, MK, MT, NL, NO, PL, PT, RO, RS, SE, SI, SK, SM, TR), OAPI (BF, BJ, CF, CG, CI, CM, GA, GN, GQ, GW, KM, ML, MR, NE, SN, TD, TG).

Published:

— *with international search report (Art. 21(3))*

SUBSTITUTED BENZOFURAN DERIVATIVES AS NOVEL ANTIMYCOBACTERIAL AGENTS

STATEMENT OF GOVERNMENT INTEREST

The present invention was developed using funding from the National Institutes of Health, Grant No. P01AI095208. The United States government has certain rights in the invention.

TECHNICAL FIELD

The present disclosure relates to compositions for inhibition of polyketide synthase 13 ("Pks 13"), and for inhibition of pathogenic bacteria expressing Pks 13, including, but not limited to, *Mycobacterium tuberculosis* ("Mtb"). Certain embodiments of the present disclosure relate to compositions comprising one or more benzofuran derivatives for inhibition of Mtb, and methods of inhibiting *Mycobacteria* comprising administering such compositions.

BACKGROUND

Tuberculosis

Tuberculosis is a common, chronic, and frequently fatal infectious disease caused by various strains of *Mycobacteria*, most commonly Mtb. Tuberculosis ("TB") causes more than 1.5 million deaths annually. Emergence of multidrug-resistant Mtb has created an urgent need for the discovery and development of new antitubercular drugs that are effective against the drug-resistant bacteria.

Over twenty drugs are currently used in various combinations for the treatment of TB. These TB drugs are classified into five groups according their effectiveness, potency, drug class and experience of use. First-line TB drugs generally have the greatest activity against TB and include isoniazid, rifampicin, pyrazinamide, ethambutol, rifapentine, and rifabutin. Second-line TB drugs are mainly reserved for the treatment of multidrug-resistant ("MDR") and X drug-resistant ("XDR") Mtb. The second-line TB drugs are generally classified into three groups, the first of which includes injectable aminoglycosides (streptomycin, kanamycin, and amikacin) and injectable polypeptides (capreomycin and viomycin), the second group including oral and injectable fluoroquinolones (ciprofloxacin, levofloxacin, moxifloxacin, ofloxacin, and

gatifloxacin), and the third including orally administered *para*-aminosalicylic acid, cycloserine, terizidone, ethionamide, prothionamide, thioacetazone, and linezolid. Third-line anti-TB drugs have unclear efficacy or undefined roles, but they can be tried as last resort drugs. Third-line anti-TB drugs and regimens include clofazimine, linezolid, amoxicillin in combination with clavulanate, imipenem in combination with cilastatin, and clarithromycin.

The current front-line therapy for TB involves a minimum of six months of intensive treatment with a four-drug combination of isoniazid, rifampicin, pyrazinamide, and ethambutol for the treatment of drug-susceptible TB. Treatment of drug-resistant TB can last for up to two years and involves the use of multiple of the second-line drugs, which have severe side effects. The duration and side effects associated with treatment of drug-resistant TB causes significant patient non-compliance, furthering the development of drug resistant *Mtb*. No single agent exists that is effective in the clinical treatment of tuberculosis, nor is there any combination of agents that offer the possibility of a therapeutic regimen having less than a six month duration. An urgent need exists for novel and potent inhibitors of pathogenic mycobacteria.

Mycolic Acid Synthesis and Pks13

Mtb has a waxy outer cell-wall layer containing extended long-chain fatty acids called mycolic acids. Mycolic acids are known to be critical for the pathogenicity, virulence, and survival of *Mtb*. Mycolic acid biosynthesis disruption is therefore an established mechanism of *Mtb* inhibition, and current front-line antitubercular drugs are known to target this biosynthetic pathway. Isoniazid, for example, targets the enoyl-acyl-ACP reductase enzyme, one of the Fatty Acid Synthase ("FAS") II system enzymes participating in the elongation of the long-chain (C_{40}-C_{60}) fatty acid components of mycolic acids. However, resistance to isoniazid is increasingly observed in clinical settings and is currently estimated at around 5% worldwide (including monoresistance, as well as MDR and XDR Mtb.

Pks 13 is a large enzyme that catalyzes condensation of two long fatty-acyl chains to synthesize mycolic acids in bacteria of the suborder *Corynebacterineae*, which includes several important human pathogens, such as *Mtb*, *Mycobacterium leprae*, and *Corynebacterium diptheriae*. In particular, Pks13 performs the final condensation of a long-chain (C_{40}-C_{60}) fatty acid (synthesized by the FAS II system) with a C_{26} fatty acid (synthesized by the FAS I system)

to form an α-hydroxy meromycolate. Pks13 is comprised of five domains that harbor all the activities required for the condensation of two long-chain fatty acids. Pks13 has two acyl carrier protein (ACP) domains, ACP_N and ACP_C, a β-ketoacyl-synthase (KS), an acyltransferase (AT) and a C-terminal thioesterase (TE) domain. The two ACP domains accept distinct substrates: the ACP_N accepts activated meroacyl-AMP from FadD32 and transfers it to the KS domain, and the ACP_C is loaded with a 2-carboxyacyl-CoA chain by the AT domain. The KS domain performs the Claisen-type condensation to produce α-alkyl β-ketoester attached to the ACP_C, which is then released by the TE domain for subsequent modification reactions.

Pks13 has been shown to be essential to *Mtb* survival and pathogenicity *in vitro*, and has been presumed to be essential *in vivo* as well. However, Pks13 is not targeted by any existing drugs in clinical use.

SUMMARY

The present disclosure relates generally to compositions and methods for inhibiting Pks13 in *Corynebacteria*, including *Mtb* in particular. In certain embodiments, the present disclosure provides one or more of: novel benzofuran derivatives; novel inhibitors of Pks13; compositions comprising a Pks13 inhibitor; methods for inhibiting a Corynebacterium; methods of inhibiting *Mtb*; and methods for inhibiting Pks13 in a pathogenic bacterium. In certain embodiments, the present disclosure provides methods for treating bacterial infections in which the pathogenic bacterium or bacteria express a Pks13 enzyme. The methods can comprise administering a Pks13 inhibitor comprising a benzofuran derivative to a patient infected with a pathogenic bacterium expressing a Pks13 enzyme.

Thus the present disclosure relates, in certain embodiments, to compositions for inhibiting a Pks13 enzyme and/or a bacterium expressing a Pks13 enzyme, including a Corynebacterium such as *Mtb*, the compositions comprising one or more benzofuran derivatives, pharmaceutically acceptable salts, hydrates, or prodrugs thereof, and combinations thereof (hereinafter, "inhibitors"). In certain embodiments in accordance with the compositions and methods of the present disclosure, the inhibitors comprise benzofuran derivatives, pharmaceutically acceptable salts, hydrates, or prodrugs thereof, and combinations thereof, the derivatives having the general structure:

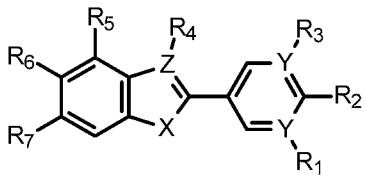

, wherein:

X is O or NH;

each Y group is independently selected from C and N;

Z is C or N;

R_1, R_2 and R_3 are independently selected from hydrogen, methoxy, hydroxyl, fluoro, nitrile, and carboxamide moieties;

R_4 is selected from the group consisting of CH_2OH, COOEt, COOH, CONHMe, CONHEt, and amides of cyclic and acyclic secondary or tertiary amines;

R_5 is an alkyl, cyclic alkyl, or heterocyclic alkyl group, optionally substituted with a substituent selected from hydroxyl, alkoxy, halogen, amine, alkylamine, hydroxyalkylamine, dialkylamine, dialkylaminealkyl, carboxy, carboxamide, acylamine, sulfoxide, sulfone, aryl, heteroaryl, and heterocyclic groups (the heretocyclic groups including, for example, morpholine, piperidine, piperizine, pyrrolidine, and azepine groups);

R_6 is selected from H, OMe, and OH; and

R_7 is selected from H, NO_2, NH_2, and NHAc.

According to certain embodiments, the disclosure provides methods of inhibiting a pathogenic bacterium expressing Pks13 by administering one or more inhibitors to the mycobacterium in an amount and for a time sufficient to inhibit the bacterium. According to certain embodiments, the disclosure provides methods of inhibiting a bacterial Pks13 enzyme by administering one or more inhibitors to the bacterium in an amount and for a time sufficient to inhibit the enzyme.

The following abbreviations and shorthand references are used throughout the specification:

Mtb - Mycobacterium tuberculosis

Pks13 - Polyketide synthase 13

TE - Thioesterase

FAS - Fatty Acid Synthase

Log - Log_{10}

4-MUH - 4-methylumbelliferyl heptanoate

Inhibitor - composition for inhibiting a mycobacterium comprising one or more benzofuran derivatives, pharmaceutically acceptable salts, hydrates, or prodrugs thereof, and combinations thereof.

BRIEF DESCRIPTION OF THE DRAWINGS

The patent or application file contains at least one drawing executed in color. Copies of this patent or patent application publication with color drawing(s) will be provided by the Office upon request and payment of the necessary fee.

A more complete understanding of the present embodiments and advantages thereof may be acquired by referring to the following description taken in conjunction with the accompanying drawings, which depict embodiments of the present disclosure, and in which like numbers refer to similar components.

FIG. 1 is a schematic representation of the structure and catalytic site of the Pks13-TE domain showing overall folding and structural elements, with the lid domain (composed of helices α4-α9) shown in cyan and the core domain (comprised of a seven-stranded β-sheet and helices α1-α3, α11) shown in orange.

FIG. 2 is a schematic representation of the Pks13-TE domain (orange) superimposed with the *E. coli* EntF structure (white) showing conserved catalytic residues Ser1533, Aps1560 and His1699, with the hydrogen bonding network between the catalytic residues depicted in dashed lines.

FIG. 3 is a representation of molecular surface structure of the Pks13-TE domain in complex with a first-generation (test) benzofuran derivative, wherein the surface groove in the lid domain is apparent, the benzofuran derivative is shown in stick representation in magenta, the lid domain is shown in cyan, the core domain is shown in orange, and the active site residues Ser1533, Aps1560 and His1699 at the interface of the lid and core domains are shown as ball and stick figures.

FIG. 4 is a schematic representation of the binding interactions of a test benzofuran derivative with the residues from the Pks13-TE lid domain, wherein the benzofuran derivative is rendered in stick form (with C-C bonds in magenta, C-O bonds in red, and C-N bonds in blue), residues of the lid domain that interact with the benzofuran derivative rendered in stick form (with C-C bonds in yellow and C-O and C-N bonds as above), and hydrogen bond interactions are shown as black dashed lines with distances ranging from 2.4 to 3.3 Å.

FIG. 5 is a stereo representation of the test and representative benzofuran derivative compounds **C**-**F** bound to the Pks13-TE domain as observed in domain-derivative complex structures, wherein the test derivative is shown in magenta, compound **C** is shown in green, compound **D** is shown in yellow, compound **E** is shown in orange, and compound **F** is shown in blue, (compounds **C**, **D**, and **E** corresponding to compound IDs **3**, **4**, and **5**, respectively).

FIG. 6 is a graph of *in vitro* cytotoxicity profile observations of human dermal fibroblast cell growth upon exposure to the test benzofuran derivative compound and compounds B-E, I, and L (corresponding to compound IDs 2-5, 13, and 17, respectively) at various concentrations as shown.

FIG. 7 is a schematic representation of the structure of the wild-type Pks13-TE domain (shown in cyan) in complex with the test benzofuran derivative compound (shown in magenta) superimposed with the structure of the benzofuran derivative-resistance conferring D1607N Pks13-TE mutant domain (shown in yellow), with hydrogen bonding between the test compound and the wild-type Pks13-TE domain represented in dotted lines and altered hydrogen bonding between the test compound and the D1607N Pks13-TE mutant domain represented in dashed lines.

DESCRIPTION

The present disclosure relates to compositions and methods for inhibition of a bacterium. These compositions and methods are described in further detail below.

Unless otherwise indicated by the specific context of this specification, such bacterium may be any bacterium inhibited by the compositions and methods of the present disclosure. Such bacterium may be a bacterium that expresses Pks13. The bacterium can be of any bacterial species that expresses Pks13, such as any species of the suborder *Corynebacteriaea*, including

any species of the genus *Mycobacterium*, including *Mtb*. Furthermore, such bacterium may be a bacterium in a patient. The patient may be any animal. In particular, the patient may be a mammal, such as a human, a pet mammal such as a dog or cat, an agricultural mammal, such as a horse, cow, buffalo, deer, pig, sheep, or goat, or a zoo mammal. Bacterial inhibition, unless otherwise indicated by the specific context of this specification, can include killing the bacterium, such as via apoptosis or necrosis, reducing or arresting the growth of the bacterium, rendering the bacterium more susceptible to the immune system, preventing or reducing bacterial infection, reducing the number of bacteria in a patient, or otherwise negatively affecting a bacterium. The same applies, *mutatis mutandis*, to a plurality of bacteria of the same or different species.

Compositions

The compositions of the present disclosure include inhibitor compositions for inhibiting Pks13, and/or inhibiting a pathogenic bacterium expressing Pks13, such as *Mtb*. The present disclosure further includes inhibitors for use in the treatment of infection by a bacterium expressing Pks13.

Unless specified to the contrary, all reference herein to compositions, inhibitors, benzofuran derivatives, and/or compounds will include any pharmaceutically acceptable salts, hydrates, or prodrugs thereof, and/or combinations thereof. The term "pharmaceutically acceptable salt" refers to salts whose counter ion derives from pharmaceutically acceptable non-toxic acids and bases.

In certain embodiments, the inhibitors comprise one or more compounds represented by the general structure below:

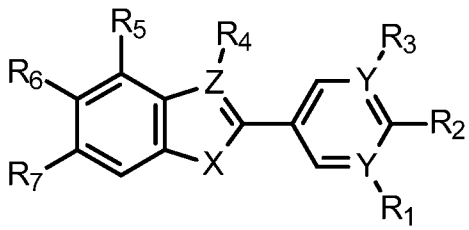

(I) , wherein:

X is O or NH;

each Y group is independently selected from C and N;

Z is C or N;

R_1, R_2 and R_3 are independently selected from hydrogen, methoxy, hydroxyl, fluoro, nitrile, and carboxamide moieties;

R_4 is selected from the group consisting of CH_2OH, COOEt, COOH, CONHMe, CONHEt, and amides of cyclic and acyclic secondary or tertiary amines;

R_5 is an alkyl, cyclic alkyl, or heterocyclic alkyl group, optionally substituted with a substituent selected from hydroxyl, alkoxy, halogen, amine, alkylamine, hydroxyalkylamine, dialkylamine, dialkylaminealkyl, carboxy, carboxamide, acylamine, sulfoxide, sulfone, aryl, heteroaryl, and heterocyclic groups (the heretocyclic groups including, for example, morpholine, piperidine, piperizine, pyrrolidine, and azepine groups);

R_6 is selected from H, OMe, and OH; and

R_7 is selected from H, NO_2, NH_2, and NHAc.

Specific compounds of the present disclosure include those having Structure I, as well as those described or characterized elsewhere herein with respect to Structure II, Structure III and Structure 4. Tables 1-7 provide a number of representative compounds of benzofuran derivative Pks13 inhibitors. The minimum inhibitory concentration ("MIC") and half-maximal inhibitory concentration ("IC_{50}") of each of the representative inhibitors is also provided. NB indicates no binding; NI indicates no inhibition, and NT indicates not tested Where incomplete inhibition was observed, percentages in square brackets indicate percentage inhibition observed, and concentrations in brackets indicate corresponding concentration.

Significant differences in potency were observed even among close structural analogs. These pharmacokinetic data are discussed in further detail below.

Benzofuran derivatives may also have the following structural formula and the R groups indicated in Table 1:

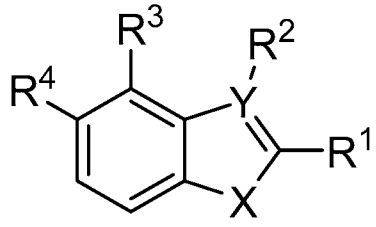

(II).

Table 1: R Groups for Structure II

ID	R^1	R^2	R^3	R^4	X	Y
1	Ph	CO_2Et	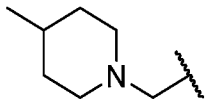	OH	O	C
2	Ph	CO_2Et	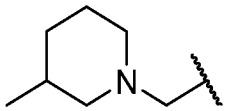	OH	O	C
3	Ph	CO_2Et	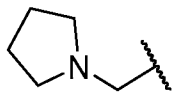	OH	O	C
4	Ph	CO_2Et	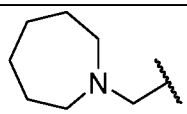	OH	O	C
5	Ph	CO_2Et	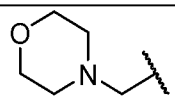	OH	O	C
109	Ph	CO_2Et	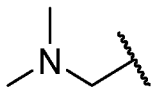	OH	O	C
6	Ph	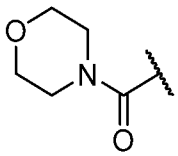	H	OH	O	C
7	Ph	CO_2Et	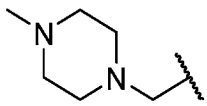	OH	O	C
8	Ph		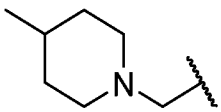	OH	NH	N
9	CH_3		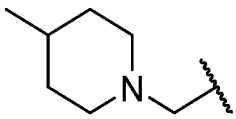	OH	NH	N
110	Ph		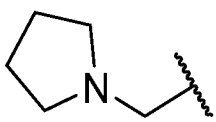	OH	NH	N

ID	R^1	R^2	R^3	R^4	X	Y
111	CH_3		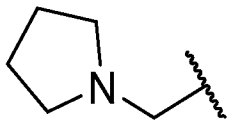	OH	NH	N

Structure II compositions also include the following composition ID 108:

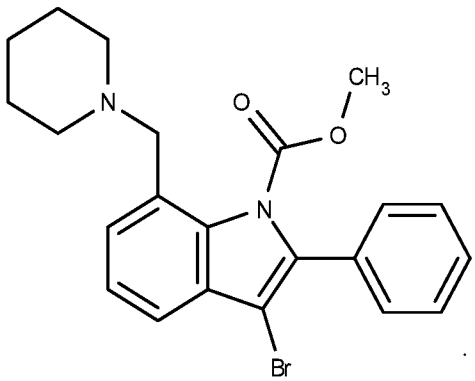

Table 2 - Structure II Pks13 Inhibition Pharmacokinetic Data

ID	*IC_{50} (μM)*	MIC *(μM)*
1	0.26±0.03	2.3±0.2
2	0.12±0.02	4.4±0.2
3	0.24±0.02	4.1
4	0.28±0.03	4.6±0.3
5	0.71±0.05	13.3±1.6
109	1.57±0.15	7.3±0.3
6	NB	NT
7	2.7	1.4
8	6.8	22

ID	*IC_{50} (μM)*	MIC *(μM)*
9	10.0	NI
110	6.8	22
111	10.0	NI
108	2	[26%] (20 μM)

Benzofuran derivatives may also have the following structural formula and the R groups indicated in Table 3:

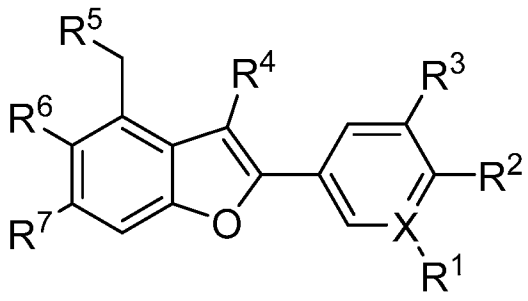

(III).

Table 3: R Groups for Structure III

ID	R^1	R^2	R^3	R^4	R^5	R^6	R^7	X
10	H	H	H	-CO_2Et	Ph	OH	H	C
12	H	H	H	-CO2Et	H	OH	H	C
13	H	H	H	-CO_2Et	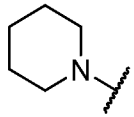	OH	H	C
14	H	H	H	-CO_2H	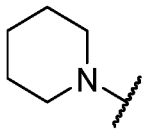	OH	H	C
15	H	H	H	-CO_2Et		OCH_3	H	C
16	H	H	H	-CO_2Et		OH	H	C
17	H	H	H	-CONHMe	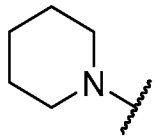	OH	H	C
18	H	H	H	-CONHEt	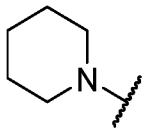	OH	H	C
19	H	H	H	-CO_2Et	Ph	OCH_3	H	C
21	H	OCH_3	H	-CO_2Et	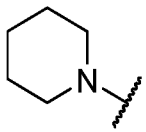	OH	H	C

ID	R^1	R^2	R^3	R^4	R^5	R^6	R^7	X
22	H	OH	H	$-CO_2Et$		OH	H	C
112	H	H	H	-CONHMe		OCH_3	H	N
24	H	H	H	$-CO_2Et$		H	H	C
25	H	F	H	$-CO_2Et$		OH	H	C
26	H	H	H	$-CO_2Et$		OH	NO_2	C
27	H	H	H	$-CO_2Et$		OH	NH_2	C
28	H	H	H	$-CO_2Et$		OH	NHAc	C

ID	R^1	R^2	R^3	R^4	R^5	R^6	R^7	X
29	H	F	H	-CONHMe		OH	H	C
31	H	OCH_3	H	-CONHMe		OH	H	C
32	H	OH	H	-CONHMe		OH	H	C
33	H	H	H	-CONHMe		H	H	C
34	H	H	H	$-CO_2Et$		H	NH_2	C
37	H	H	H	$-CO_2Et$		H	OCH_3	C
38	H	H	H	$-CO_2Et$		H	OH	C

ID	R^1	R^2	R^3	R^4	R^5	R^6	R^7	X
39	H	H	H	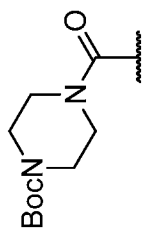	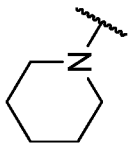	OH	H	C
40	H	H	H	-CONHMe	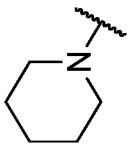	H	OH	C
41	H	H	H	-CONHMe	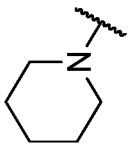	OH	H	C
42	H	H	H	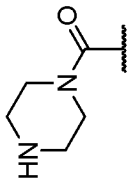	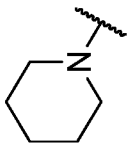	OH	H	C
43	H	H	H	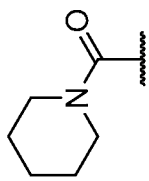	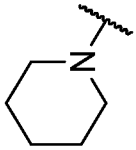	OH	H	C
44	H	H	H	-CONH$(CH_2)_2$NHAc	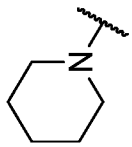	OH	H	C

ID	R^1	R^2	R^3	R^4	R^5	R^6	R^7	X
45	H	OH	H	$-CO_2Et$		H	OH	C
46	H	H	H			OH	H	C
47	H	OH	H	$-CO_2Et$		H	OH	C
48	OCH_3	H	H	$-CO_2Et$		OH	H	C
49	H	F	H	$-CO_2Et$		H	OH	C
50	OH	H	H	$-CO_2Et$		OH	H	C
51	H	F	H	$-CO_2Et$		H	OH	C

ID	R^1	R^2	R^3	R^4	R^5	R^6	R^7	X
52	H	H	H	$-CO_2Et$		OH	H	C
53	H	H	H			OH	H	C
54	H	H	H			OH	H	C
56	OCH_3	H	H	-CONHMe		OH	H	C
57	OH	H	H	-CONHMe		OH	H	C
58		OH	H	$-CO_2Et$		OH	H	N
59	F	OH	H	$-CO_2Et$		OH	H	C

ID	R^1	R^2	R^3	R^4	R^5	R^6	R^7	X
60	H	$CONH_2$	H	$-CO_2Et$		OH	H	C
61	F	OH	H	-CONHMe		OH	H	C
62	H	CN	H	$-CO_2Et$		OH	H	C
63	F	OH	F	$-CO_2Et$		OH	H	C
64	F	OH	F	-CONHMe		OH	H	C
65	H	H	H	$-CH_2OH$		OH	H	C
116	H	H	H	$-CO_2Et$		OH	H	C

ID	R^1	R^2	R^3	R^4	R^5	R^6	R^7	X
117	H	H	H	$-CO_2Et$		OH	H	C
118	H	OH	H	-CONHMe		OH	H	C
119	H	H	H	$-CO_2Et$		OH	H	C
120	H	OH	H	-CONHMe		OH	H	C
121	H	OH	H	-CONHMe		OH	H	C
122	H	OH	H	-CONHMe		OH	H	C
123	H	OH	H	-CONHMe		OH	H	C

ID	R^1	R^2	R^3	R^4	R^5	R^6	R^7	X
124	H	OH	H	-CONHMe	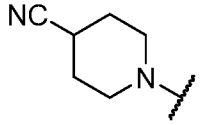	OH	H	C
125	H	OH	H	$-CONH_2$	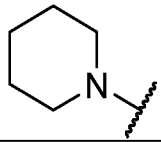	OH	H	C
126	H	OH	H	-CONHMe	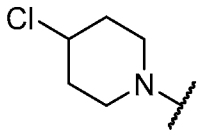	OH	H	C
127	H	OH	H	-CONHMe	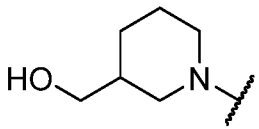	OH	H	C
128	H	OH	H	-CONHMe	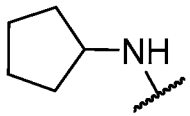	OH	H	C
129	H	OH	H	-CONHMe	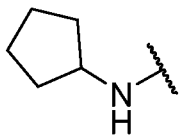	H	H	C
130	H	H	H	$-CO_2Et$	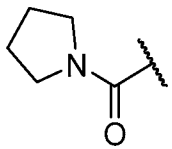	OH	H	C

ID	R^1	R^2	R^3	R^4	R^5	R^6	R^7	X
131	H	H	H	$-CO_2Et$		OH	H	C
132	H	H	H	$-CO_2Et$		OH	H	C
133	H	H	H	$-CO_2Et$		OH	H	C
134	H	OH	H	$-CO_2Et$		OH	H	C
135	H	H	H	-CONHMe		OH	H	C
67	H	H	H	$-CO_2Et$		H	OH	C

ID	R^1	R^2	R^3	R^4	R^5	R^6	R^7	X
68	H	H	H	-CONHMe	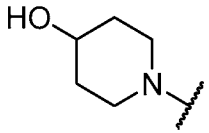	H	OH	C
69	H	H	H	$-CO_2Et$	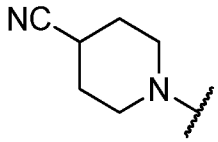	H	OH	C
70	H	H	H	$-CO_2Et$	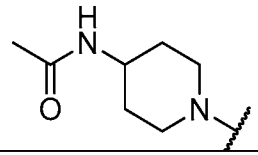	H	OH	C
72	H	H	H	$-CO_2Et$	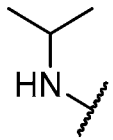	H	OMe	C

Table 4: Other Structure III Compositions

ID	Structure
11	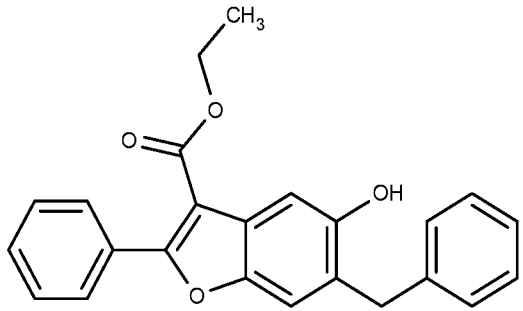

ID	Structure
71	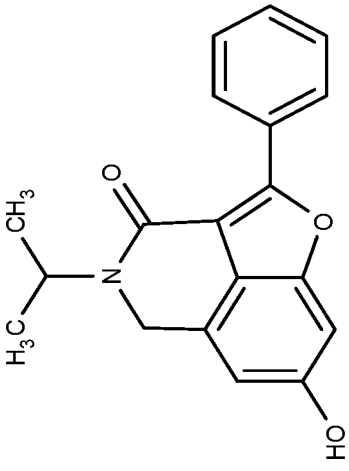
20	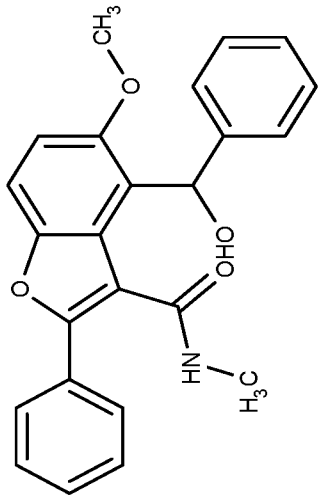
30	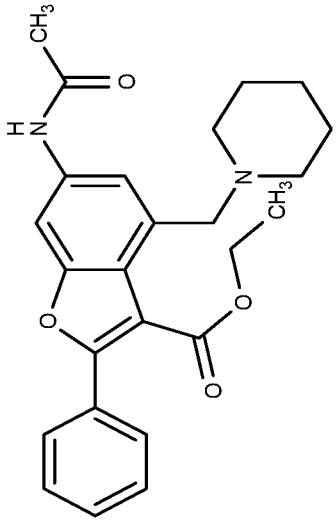
23	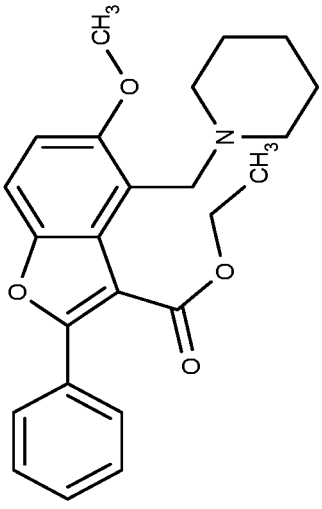
35	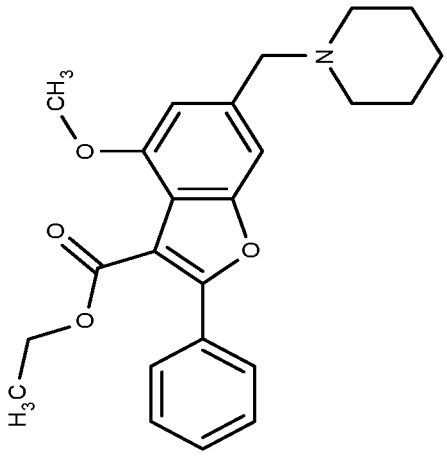
55	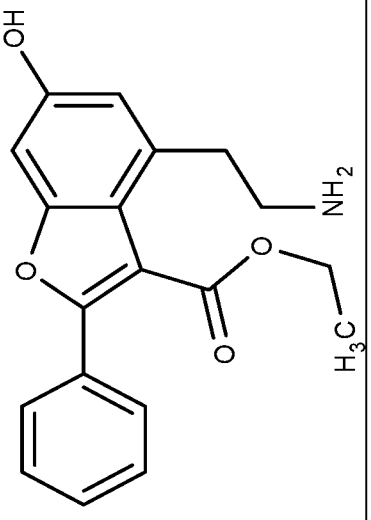

ID	Structure
83	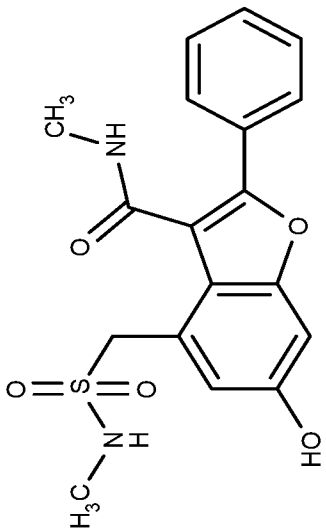
84	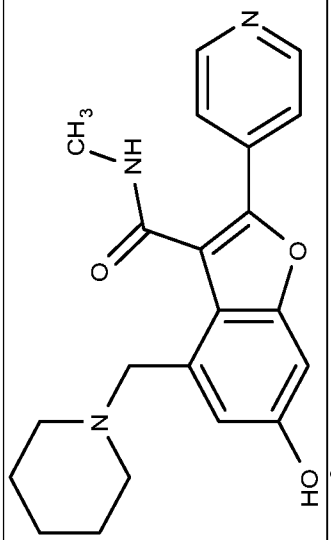
85	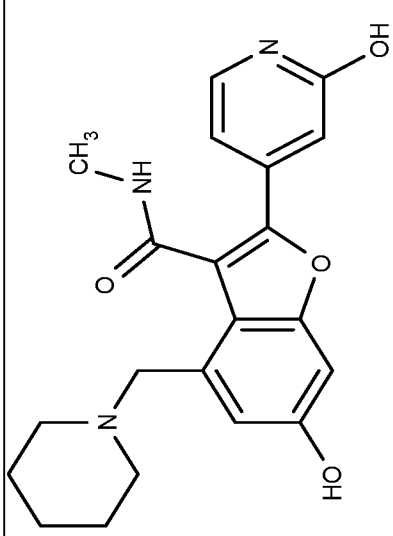

ID	Structure
36	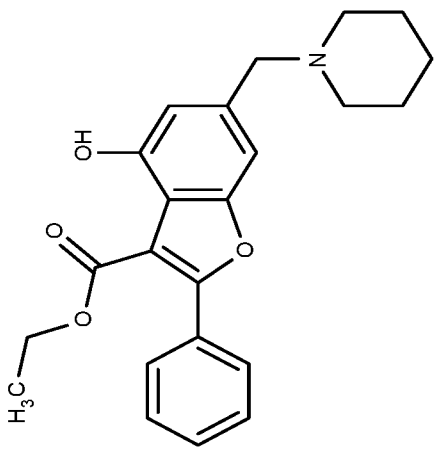
66	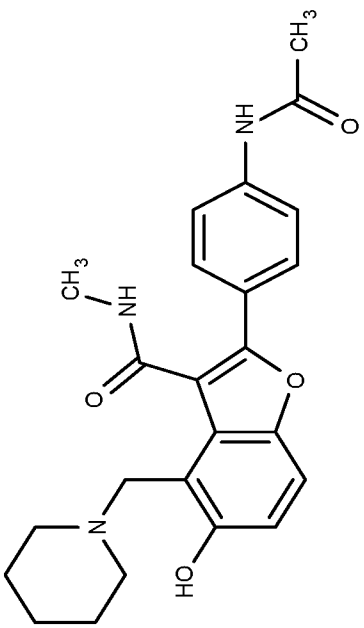
82	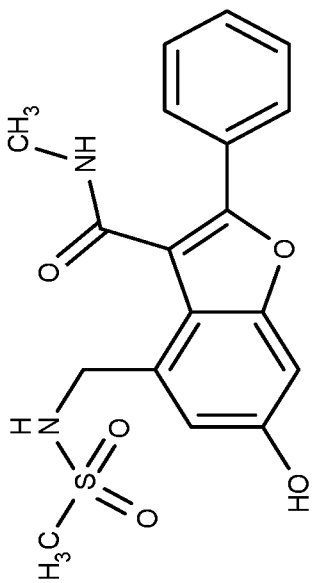

ID	Structure
93	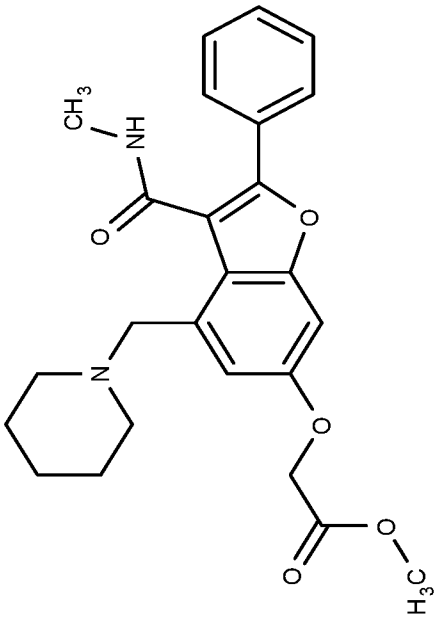
86	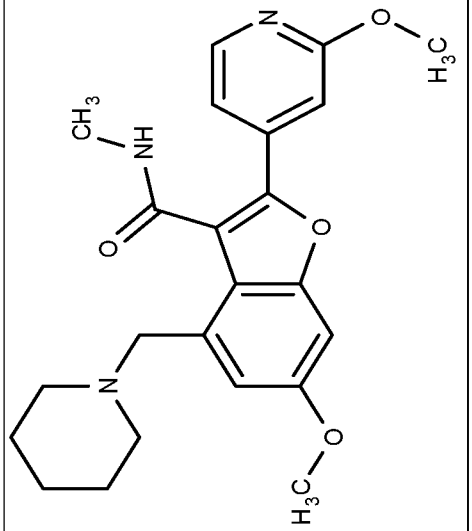

ID	Structure
87	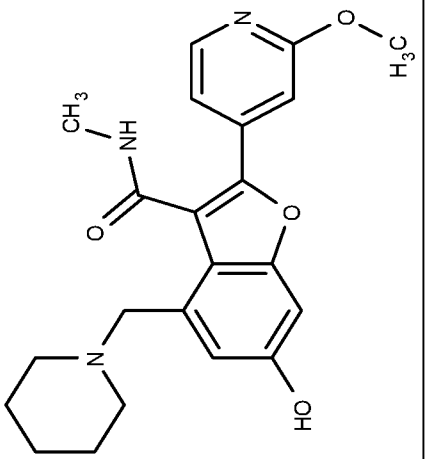
89	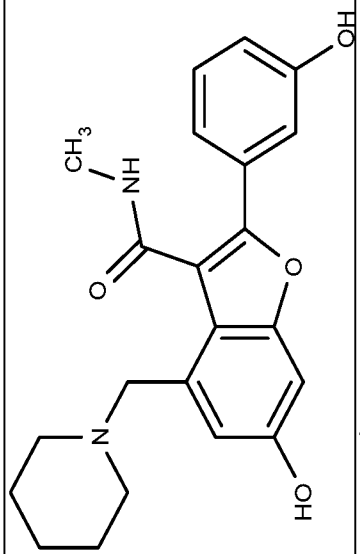
91	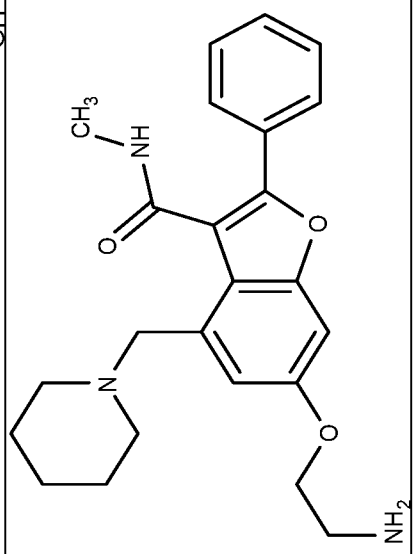

ID	Structure
94	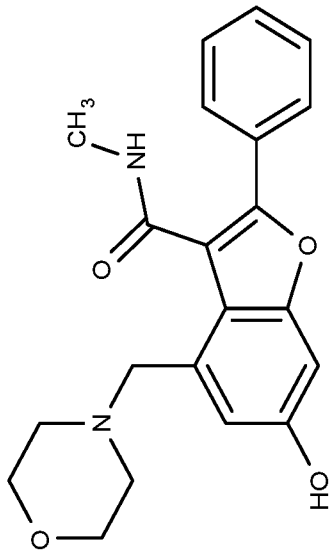
95	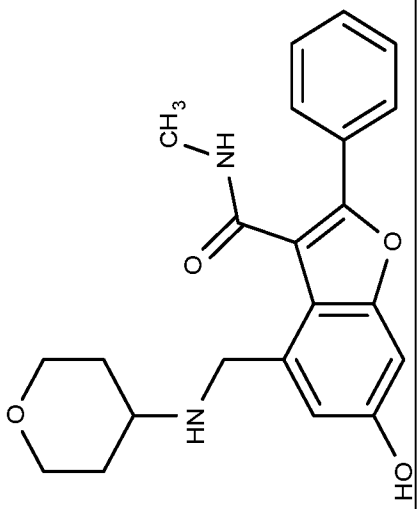
96	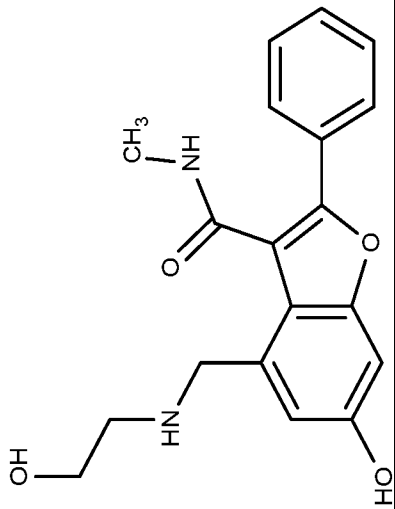

ID	Structure
88	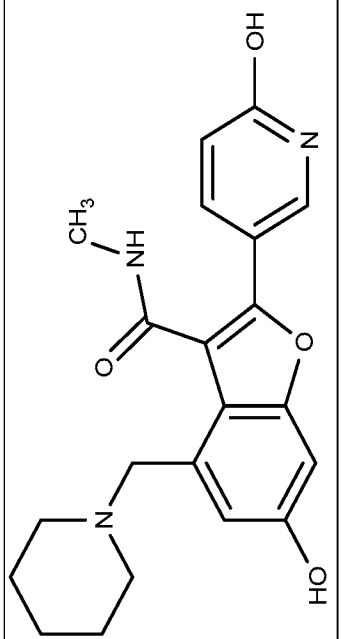
90	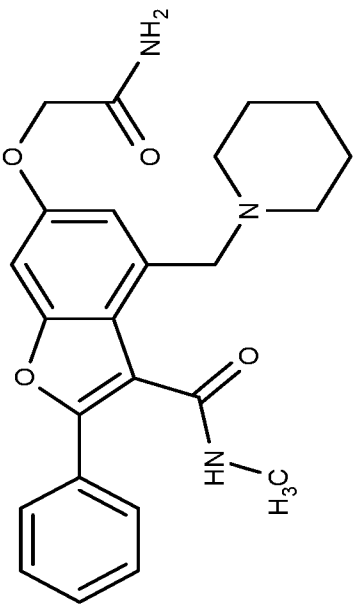
92	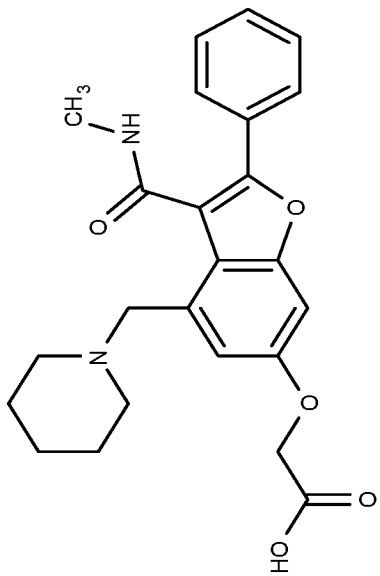

ID	Structure
103	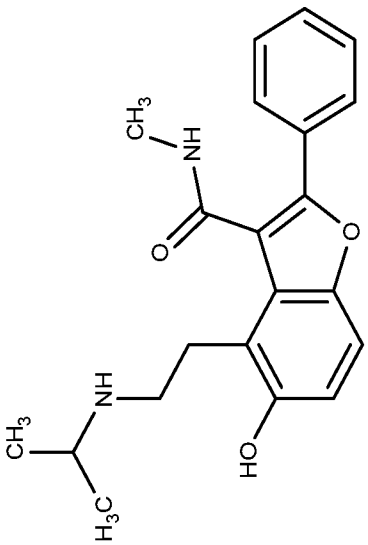
105	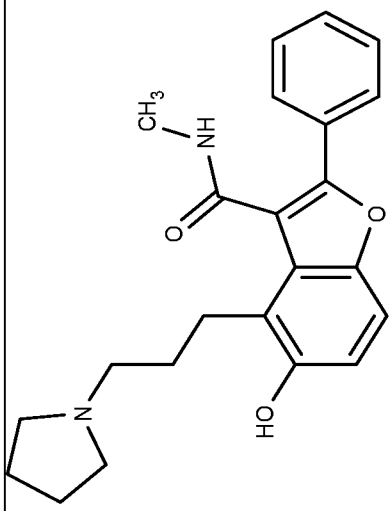
98	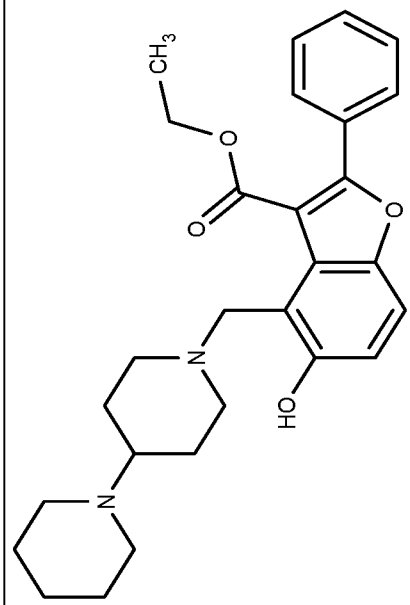
97	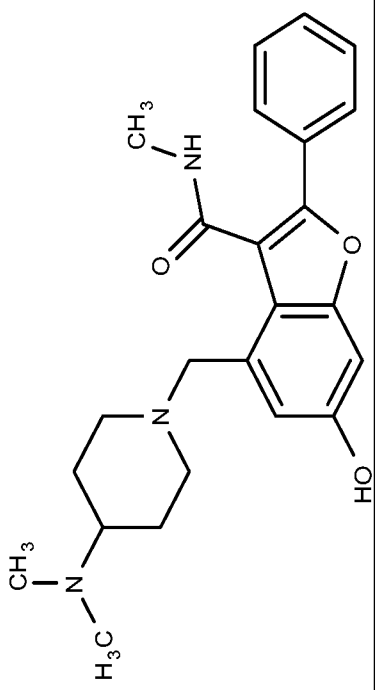
99	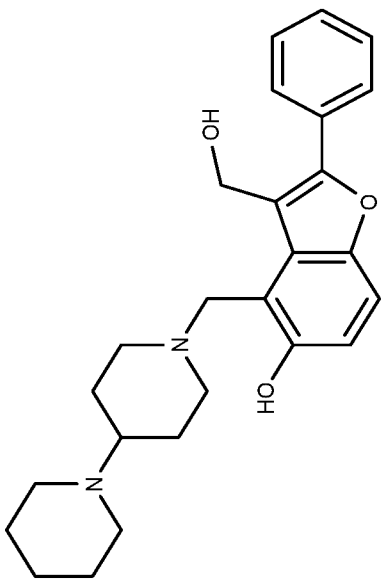
101	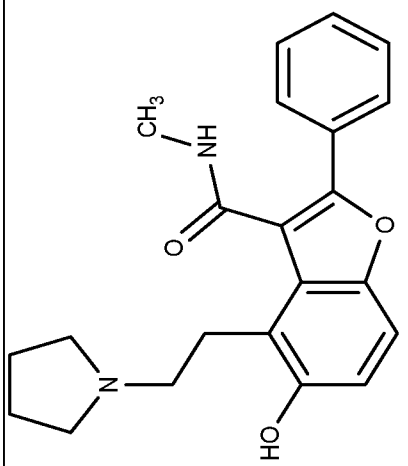

ID	Structure
104	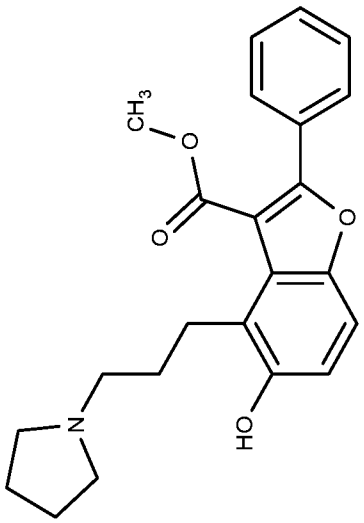
106	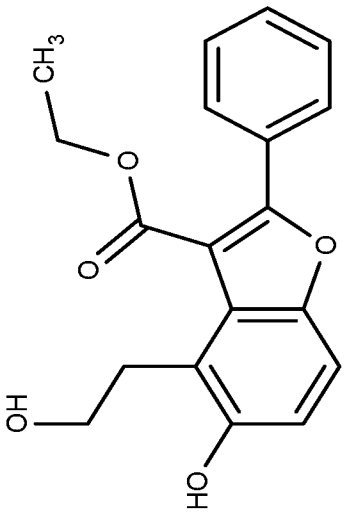
107	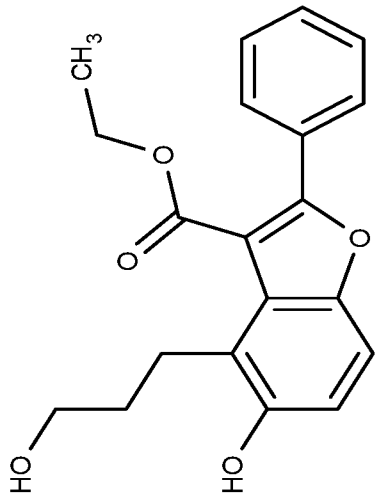

ID	Structure
100	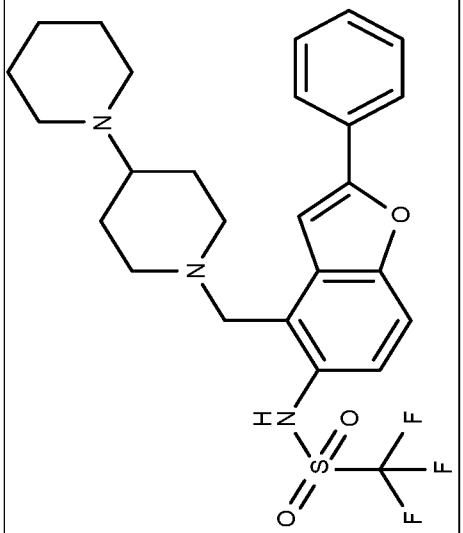
102	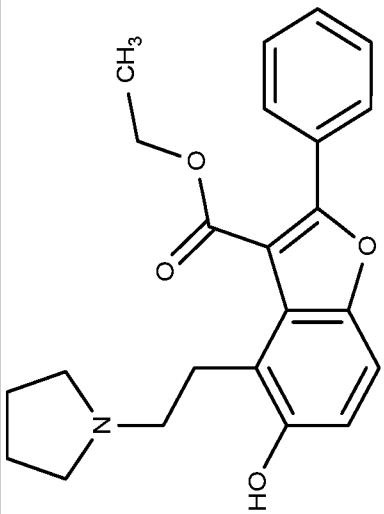

Table 5: Structure III Pks13 Inhibition Pharmacokinetic Data

ID	IC_{50} (μM)	MIC (μM)
10	11.9	40
12	>20	20
13	0.26	0.4
14	6.6	NI
15	NB	NI
16	19.6	5.2
17	0.29	2
18	0.36	14
19	50.0	50
21	0.29	2.6
22	0.19	0.6
112	35.8	>40
24	2.0	16

ID	IC_{50} (μM)	MIC (μM)
25	0.35	1.5
26	1.3	5.4
27	0.37	8
28	3.1	20
29	0.3	4.5
31	0.26	1.1
32	0.19	0.09
33	45	>50
34	4.5	9.2
37	29	7.3
38	0.45	6.7
39	0.66	2.1
40	0.6	20

ID	IC_{50} (μM)	MIC (μM)
41	0.44	20
42	0.74	3.1
43	0.32	>10
44	0.5	>40
45	0.44	1.1
46	0.34	>20
47	0.57	1.0
48	0.36	1.3
49	0.4	>10
50	0.23	0.23
51	0.8	>30
52	>20	NT
53	0.63	6.6

ID	IC_{50} (μM)	MIC (μM)
54	5.3	20
56	0.4	9.0
57	0.27	0.44
58	0.36	4.0
59	0.29	0.3
60	0.3	3.5
61	0.33	0.5
62	0.27	1.5
63	0.5	7.0
64	1.5	>40
65	0.24	12.5
116	NA	NA
117	0.18	5.6
118	0.48	5.0

ID	IC_{50} (μM)	MIC (μM)
119	0.8	NA
120	0.5	4.2
121	0.6	40
122	0.51	1.0
123	1.6	>40
124	0.25	20
125	0.17	1.3
126	NA	NA
127	1.1	5.0
128	1.0	1.0
129	NA	NA
130	NA	4.1
131	NA	7.2
132	0.42	10

ID	IC_{50} (μM)	MIC (μM)
133	>10	NT
134	0.4	2.5
135	2.0	0.5
67	0.70	9.0
68	>20	NT
69	1.6	20
70	6.1	>40
72	>10	7.4
11	NT	28
23	NT	35.8
35	NT	40
55	4	> 20
71	9	>20
20	50	50

ID	IC_{50} (μM)	MIC (μM)
30	NT	20-27
36	NT	40
66	NT	> 20
82	NT	NI
83	NT	>20
84	NT	6.1
85	NT	> 10
87	NT	3.3
89	9	1.2
91	10	[34%] (40 μM)

ID	IC_{50} (μM)	MIC (μM)
93	10	[16%] (40 μM)
86	> 20	>20
88	NT	2.8
90	[31%] (40 μM)	[13%] (20 μM)
92	INS	INS
94	NT	> 20
95	NT	8
96	NT	9
97	NT	NI
99	NI	[28%] (20 μM)

ID	IC_{50} (μM)	MIC (μM)
101	10	3.3
103	>20	0.45
105	5	5
98	>20	[40%] (20 μM)
100	>40	[6%] (20 μM)
102	2.5	0.7
104	2	1.8
106	NT	> 20
107	NT	> 20

Benzofuran derivatives may also have the following structural formula and the R groups indicated in Table 6:

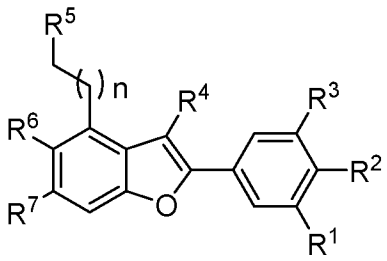

(IV).

Table 6: R Groups for Structure IV

ID	R^1	R^2	R^3	R^4	R^5	R^6	R^7	*n*
136	H	H	H	-CO_2Et	NH_2	H	OH	1
137	H	H	H	-CONHMe	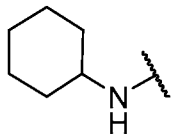	OH	H	1
138	H	H	H	-CONHMe	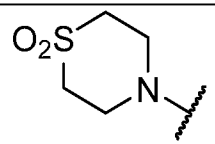	OH	H	1
139	H	H	H	-CONHMe	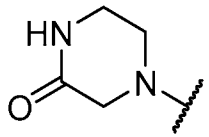	OH	H	1
140	H	H	H	-CONHMe	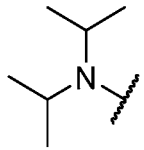	OH	H	1
141	H	H	H	-CONHMe	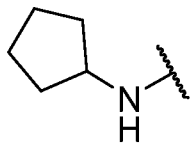	OH	H	1
142	H	H	H	-CONHMe	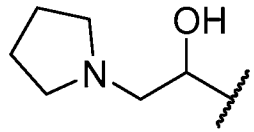	OH	H	1

ID	R^1	R^2	R^3	R^4	R^5	R^6	R^7	*n*
143	H	H	H	-CONHMe	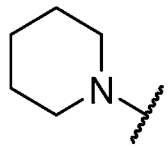	OH	H	1
144	H	H	H	-CONHMe	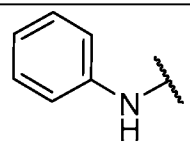	OH	H	1
145	H	H	H	-CONHMe	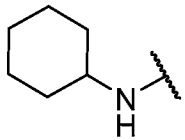	OH	H	1
146	H	H	H	-CONHMe	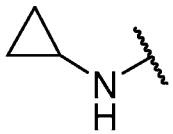	OH	H	1
147	H	H	H	-CONHMe	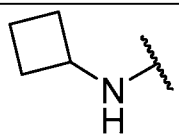	OH	H	1
148	H	H	H	-CO_2H	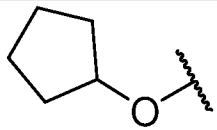	OH	H	1
149	H	H	H	-CO_2Et	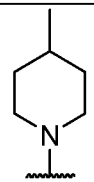	OH	H	1

ID	R^1	R^2	R^3	R^4	R^5	R^6	R^7	*n*
150	H	H	H	-CO_2Et	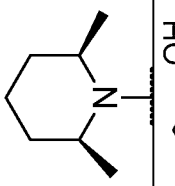	OH	H	1
151	H	H	H	-CO_2Et	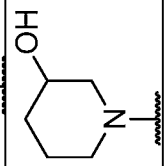	OH	H	1
152	H	H	H	-CONHMe	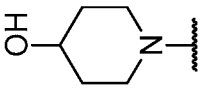	OH	H	1
153	H	H	H	-CONHMe	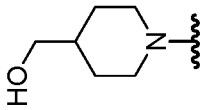	OH	H	1
154	H	H	H	-CONHMe	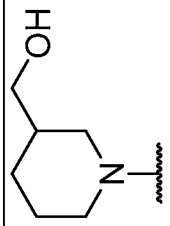	OH	H	1

ID	R^1	R^2	R^3	R^4	R^5	R^6	R^7	n
155	H	H	H	-CONHMe		OH	H	1
156	H	H	H	-CONHMe		OH	H	1
157	H	H	H	-CONHMe		OH	H	1
158	H	H	H	-CONHMe		OH	H	1
159	H	H	H	-CONHMe		OH	H	1
160	H	H	H	-CONHMe		OH	H	2

ID	R^1	R^2	R^3	R^4	R^5	R^6	R^7	*n*
161	H	H	H	-CO2Et		OH	H	2
162	H	H	H	-CO_2Et		OH	H	2
163	H	H	H	-CONHMe		OH	H	2
164	H	H	H	-CO_2Et		OH	H	2

ID	R^1	R^2	R^3	R^4	R^5	R^6	R^7	*n*
165	H	H	H	-CO_2Et	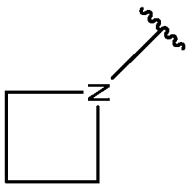	OH	H	2
166	H	H	H	-CO_2Et	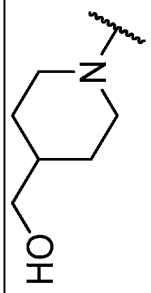	OH	H	2
167	H	H	H	-CONHMe	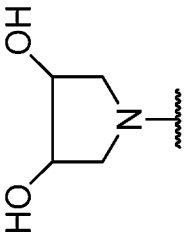	OH	H	1
168	H	H	H	-CONHMe	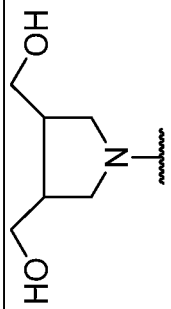	OH	H	1
169	H	H	H	-CO_2Et	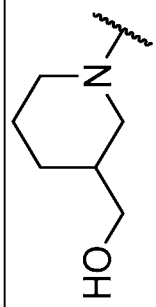	OH	H	2
170	H	H	H	-CO_2Et	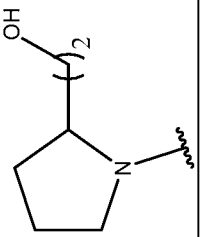	OH	H	2

ID	R^1	R^2	R^3	R^4	R^5	R^6	R^7	*n*
171	H	H	H	-CO_2Et	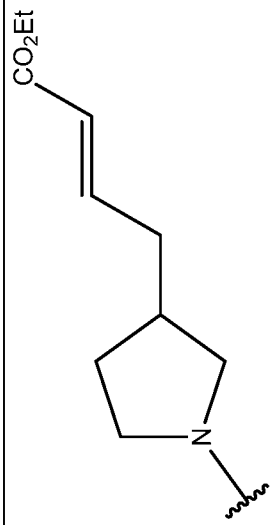	OH	H	2
172	H	H	H	-CO_2Et	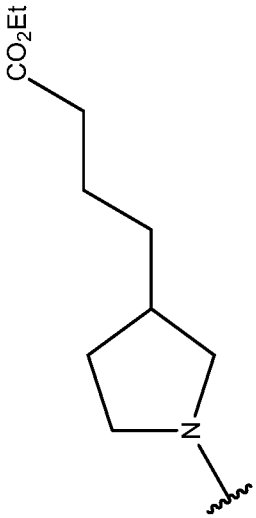	OH	H	2
173	H	H	H	-CO_2Et	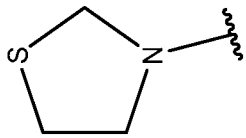	OH	H	2
174	H	H	H	-CO_2Et	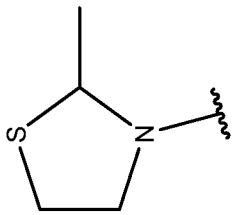	OH	H	2

ID	R^1	R^2	R^3	R^4	R^5	R^6	R^7	*n*
175	H	H	H	-CO_2Et	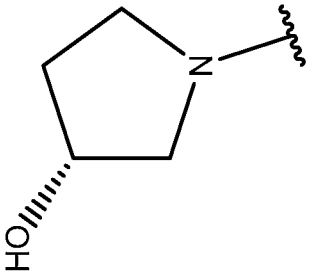	OH	H	2
176	H	H	H	-CO_2Et	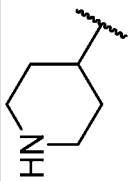	OH	H	1
177	H	H	H	-CO_2Et	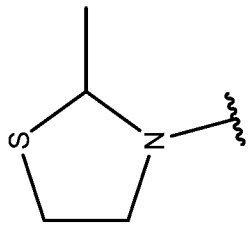	OH	H	1
178	H	H	H	-CO_2Et	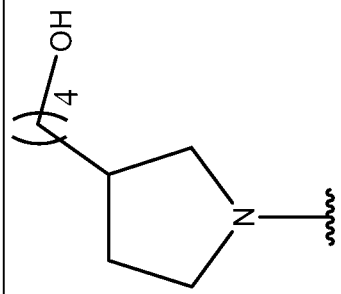	OH	H	1

ID	R^1	R^2	R^3	R^4	R^5	R^6	R^7	*n*
179	H	H	H	-CO_2Et		OH	H	1
180	H	H	H	-CO_2Et		OH	H	2
181	H	H	H	-CO_2Et		OH	H	2
182	H	H	H	-CONHMe		H	OH	2

ID	R^1	R^2	R^3	R^4	R^5	R^6	R^7	*n*
183	H	H	H	$-CO_2Et$	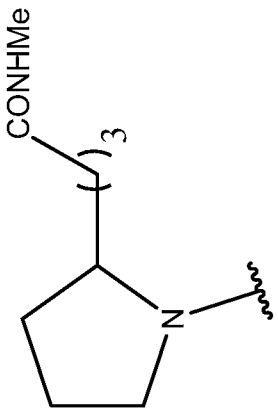	OH	H	2
184	H	H	H	$-CO_2Et$	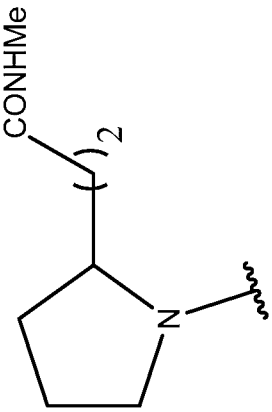	OH	H	2
185	H	H	H	$-CO_2Et$	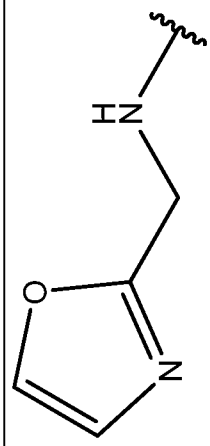	OH	H	1
186	H	H	H	$-CO_2Et$	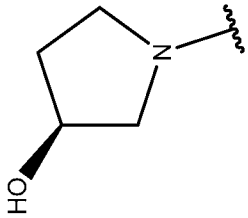	OH	H	2

ID	R^1	R^2	R^3	R^4	R^5	R^6	R^7	*n*
187	H	H	H	-CO_2Et	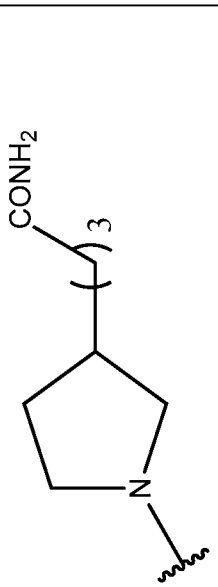	OH	H	1
188	H	H	H	-CO_2Et	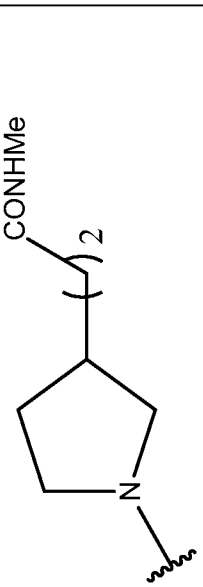	OH	H	1
189	H	H	H	-CO_2Et	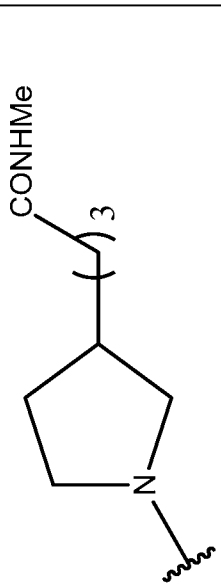	OH	H	2
190	H	H	H	-CONHMe	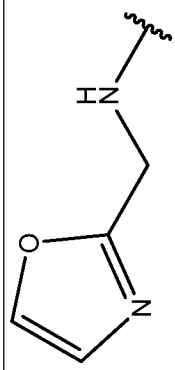	OH	H	2
191	H	H	H	-CO_2Et	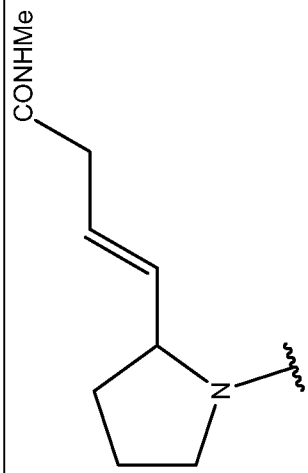	OH	H	2

ID	R^1	R^2	R^3	R^4	R^5	R^6	R^7	*n*
192	H	H	H	-CO_2Et	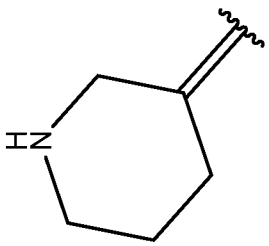	OH	H	1
193	H	H	H	-CO_2Et	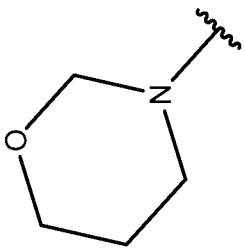	OH	H	1
194	H	H	H	-CONHMe	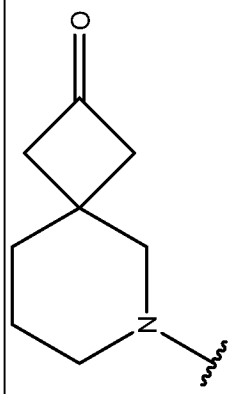	OH	H	2
195	H	H	H	-CONHMe	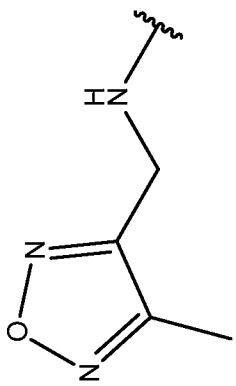	OH	H	2

ID	R^1	R^2	R^3	R^4	R^5	R^6	R^7	*n*
196	H	H	H	-CONHMe		OH	H	2
197	H	H	H	$-CO_2Et$		OH	H	2
198	H	H	H	$-CO_2Et$		OH	H	2
199	H	H	H	$-CO_2Et$		OH	H	2
200	H	H	H	-CONHMe		OH	H	2
201	H	OH	H	$-CO_2Et$		OH	H	2

ID	R^1	R^2	R^3	R^4	R^5	R^6	R^7	*n*
202	H	OH	H	-CONHMe	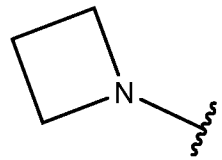	OH	H	2
203	H	H	H	-CONHMe	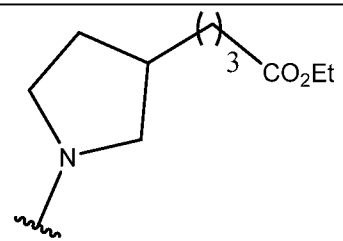	OH	H	2
204	H	OH	H	-CONHMe	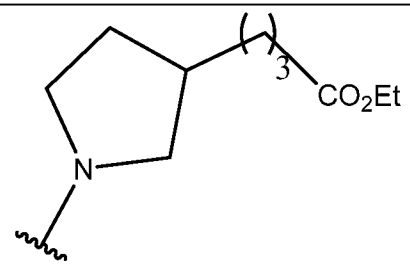	OH	H	2
205	H	H	H	-CONHMe	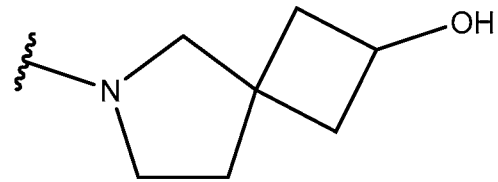	OH	H	2
206	H	H	H	-CONHMe	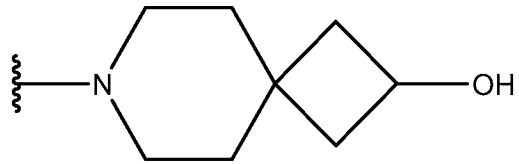	OH	H	2

ID	R^1	R^2	R^3	R^4	R^5	R^6	R^7	*n*
207	H	H	H	-CONHMe	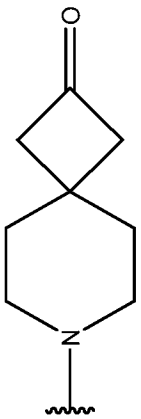	OH	H	2
208	H	OH	H	$-CONMe_2$	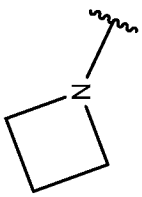	H	OH	2
209	H	OH	H	$-CONMe_2$	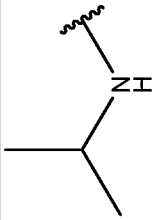	OH	H	1
210	H	OH	H	$-CONMe_2$	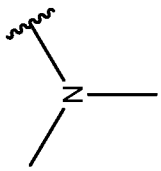	OH	H	1
211	H	H	H	$-CONH^iPrMe$	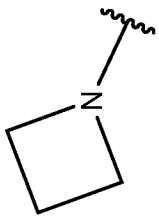	OH	H	2
212	H	H	H	$-CO_2Et$	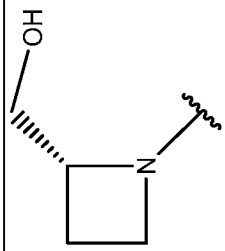	OH	H	2

ID	R^1	R^2	R^3	R^4	R^5	R^6	R^7	*n*
213	H	H	H	-CO_2Et		OH	H	2
214	H	OH	H	-CONH^{i}Pr		OH	H	2
215	H	H	H	-CO_2Et		OH	H	3
216	H	H	H	-CO_2H		OH	H	2
217	H	OH	H			OH	H	2
218	H	H	H	-CO_2Et		OH	H	2

ID	R^1	R^2	R^3	R^4	R^5	R^6	R^7	*n*
219	H	H	H	-CO_2Et		OH	H	2
220	H	H	H	-CO_2Et		OH	H	1
221	H	H	H	-CO_2Et		OH	H	1
222	H	OH	H	-CONHMe		OH	H	2

ID	R^1	R^2	R^3	R^4	R^5	R^6	R^7	*n*
223	H	OH	H	-CONHEt		OH	H	2
224	H	OH	H	$-CONHCH_2CF_3$		OH	H	2
73	H	F	H	$-CO_2Et$		H	OH	1
74	H	F	H	$-CO_2Et$		H	OH	1
75	H	F	H	$-CO_2Et$		H	OH	1
76	H	F	H	$-CH_2OH$		H	OH	1
77	H	F	H	$-CO_2Et$		H	OH	1

ID	R^1	R^2	R^3	R^4	R^5	R^6	R^7	*n*
78	H	F	H	-CO_2Et		H	OH	1
79	H	F	H	-CO_2Et		H	OH	1
80	H	F	H	-CO_2Et		H	OH	1
81	H	F	H	-CO_2Et		H	OH	1
225	H	F	H	-CO_2Et		H	OH	1
226	H	F	H	-CO_2Et		H	OH	1
227	H	H	H	-CO_2Et		OH	H	1

ID	R^1	R^2	R^3	R^4	R^5	R^6	R^7	*n*
228	H	H	H	-CO_2Et		OH	H	1
229	H	H	H	-CO_2Et		OH	H	1
230	H	H	H	-CONHMe		OH	H	1
231	H	H	H	-CONHMe		OH	H	1
232	H	H	H	-CONHMe		OH	H	1
233	H	H	H	-CONHMe		OH	H	1
234	H	H	H	-CONHMe		OH	H	1

ID	R^1	R^2	R^3	R^4	R^5	R^6	R^7	*n*
235	H	H	H	-CONHMe	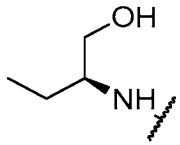	OH	H	1
236	H	H	H	$-CO_2Et$	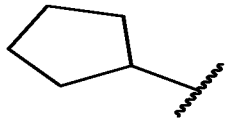	OH	H	2
237	H	H	H	-CONHMe	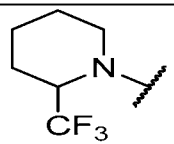	OH	H	1
238	H	H	H	-CONHMe	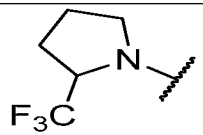	OH	H	1
239	H	H	H	-CONHMe	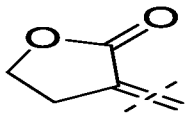	OH	H	1
240	H	H	H	-CONHMe	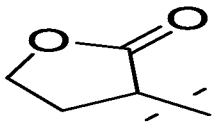	OH	H	1
241	H	H	H	$-CO_2Et$	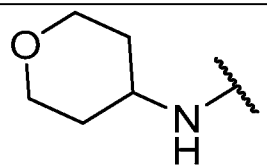	OH	H	1
242	H	F	H	$-CO_2Et$	NH_2	H	OH	1

ID	R^1	R^2	R^3	R^4	R^5	R^6	R^7	*n*
243	H	F	H	-CO_2Et	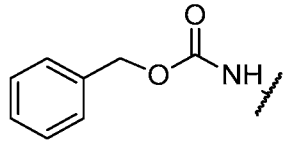	H	OH	1
244	H	H	H	-CO_2Et	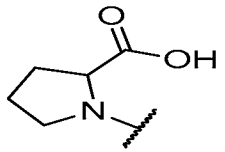	OH	H	1
245	H	H	H	-CO_2Et	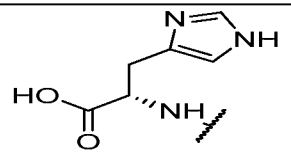	OH	H	1
246	H	H	H	-CO_2Et	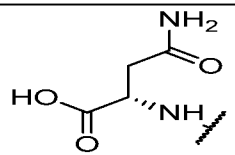	OH	H	1
247	H	H	H	--CO_2Et	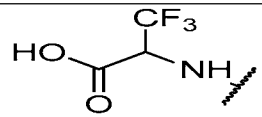	OH	H	1
248	H	H	H	-CO_2Et	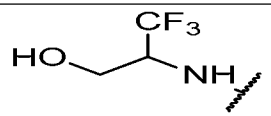	OH	H	1
249	H	H	H	-CO_2Et	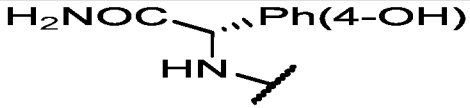	OH	H	1

ID	R^1	R^2	R^3	R^4	R^5	R^6	R^7	*n*
250	H	H	H	-CONHMe		OH	H	1
251	H	H	H	-CONHMe		OH	H	1
252	H	H	H	-CONHMe		OH	H	1
253	H	H	H	-CONHMe		OH	H	1
254	H	H	H	$-CO_2Et$		OH	H	1
255	H	H	H	$-CO_2Et$		OH	H	2
256	H	H	H	$-CO_2Et$		OH	H	1

ID	R^1	R^2	R^3	R^4	R^5	R^6	R^7	*n*
257	H	H	H	-CONHMe		OH	H	1
258	H	H	H	-CONHMe		OH	H	1
259	H	H	H	-CONHMe		OH	H	1
260	H	H	H	-CONHMe		OH	H	1
261	H	F	H	-CONHMe		H	OH	1
262	H	F	H	-CONHMe		H	OH	1

ID	R^1	R^2	R^3	R^4	R^5	R^6	R^7	*n*
263	H	H	H	-CONHMe		OH	H	1
264	H	H	H	$-CO_2Et$		OH	H	1
265	H	H	H	-CONHMe		OH	H	1
266	H	H	H	$-CO_2Et$		OH	H	1
267	H	H	H	$-CO_2Et$		OH	H	1
268	H	H	H	-CONHMe		OH	H	1
269	H	H	H	$-CO_2Et$		OH	H	1

ID	R^1	R^2	R^3	R^4	R^5	R^6	R^7	*n*
270	H	H	H	-CO_2Et		OH	H	1
271	H	H	H	-CONHMe		OH	H	2
272	H	H	H	-CO_2Et		OH	H	1
273	H	H	H	-CO_2Et		OH	H	1
274	H	H	H	-CONHMe		OH	H	1
275	H	H	H	-CONHMe		OH	H	1

Table 7: Structure IV and Pks13 Inhibition Pharmacokinetic Data

ID	IC_{50} (μM)	MIC (μM)
136	>20	4
137	NA	NA
138	>40	NT
139	>40	NT
140	>40	NT
141	1.4	10.0
142	40	NT
143	>20	NT
144	>40	NT
145	10.0	NA
146	NA	NA
147	3.5	NA
148	NA	NA

ID	IC_{50} (μM)	MIC (μM)
149	10	2.3
150	>40	NT
151	10	>20
152	>40	NT
153	>40	NT
154	>20	NT
155	>40	NT
156	>40	NT
157	>40	NT
158	20	NT
159	20	NT

ID	IC_{50} (μM)	MIC (μM)
160	10	NT
161	0.8	1.0
162	2.7	2.5
163	>40	NT
164	NA	NA
165	0.8	0.08
166	0.5	6.1
167	NA	NA
168	20.0	NT
169	>40	NT

ID	IC_{50} (μM)	MIC (μM)
170	4.3	NA
171	0.5	2.7
172	0.7	2.9
173	5.0	NA
174	1.25	4.7
175	0.95	6.1
176	>40	NT
177	1.0	NA
178	2.0	NA
179	6.5	NA
180	1.9	NA
181	2.5	NA

ID	IC_{50} (μM)	MIC (μM)
182	NA	NA
183	NA	NA
184	>10	NT
185	NA	NA
186	0.62	10
187	0.5	NA
188	NA	NA
189	10.0	NT
190	>40	NT
191	20	NT
192	>40	NT
193	5.0	NA

ID	IC_{50} (μM)	MIC (μM)
194	>40	NT
195		>40
196	>20	NT
197	7.5	NA
198	5	NA
199	2.5	1.2
200	4.4	0.6
201	2.1	<0.08
202	1.6	15
203	NA	NA
204	NA	NA
205	NA	NA
206	NA	NA

ID	IC_{50} (μM)	MIC (μM)
207	10	NT
208	4.0	NA
209	1.8	0.45
210	12	NT
211	NA	0.33
212	1.94	1.1
213	2.3	0.97
214	NA	<0.08
215	NA	<0.08
216	NA	NA
217	NA	NA
218	NA	2.8
219	NA	NA

ID	IC_{50} (μM)	MIC (μM)
220	NA	NA
221	NA	NA
222	NA	NA
223	NA	NA
224	NA	NA
73	2.1	2.5
74	20	NT
75	>20	NT
76	>20	NT
77	6	3.3
78	13.0	NT
79	>20	NT
80	>40	NT
81	>40	NT

ID	IC_{50} (μM)	MIC (μM)
225	>40	NT
226	>40	NT
227	>20	NT
228	3.6	5.0
229	5.8	3.2
230	40	NT
231	5.0	8.0
232	>20	NT
233	>10	NT
234	5.3	>20
235	2.3	>40
236	>10	NT
237	>20	NT
238	40	NT

ID	IC_{50} (μM)	MIC (μM)
239	10	NT
240	>40	NT
241	>20	NT
242	>20	NT
243	>40	NT
244	>40	20-40
245	2.7	>40
246	20	NT
247	>40	NT
248	20	NT
249	>40	NT
250	2.4	NA
251	1.6	NA

ID	IC_{50} (μM)	MIC (μM)
252	1.6	NA
253	0.8	NA
254	2.7	NA
255	2.1	NA
256	1.5	NA
257	1.25	NA
258	2.5	NA
259	1.0	NA
260	4.0	NA
261	5.0	5.0
262	>40	NT
263	10	NT
264	2.5	NT

ID	IC_{50} (μM)	MIC (μM)
265	0.3-.0.6	NT
266	10.0	NT
267	>40	NT
268	40	NT
269	NA	NA
270	NA	NA
271	7.0	NT
272	NA	NA
273	NA	NA
274	NA	NA
275	NA	NA

Benzofuran derivatives which contain a basic moiety, such as, but not limited to an amine or a pyridine or imidazole ring, may form salts with a variety of organic and inorganic acids. Suitable pharmaceutically acceptable (i.e., non-toxic, physiologically acceptable) base addition salts for the compounds of the present invention include inorganic acids and organic acids. Examples include acetate, adipate, alginates, ascorbates, aspartates, benzenesulfonate (besylate), benzoate, bicarbonate, bisulfate, borates, butyrates, carbonate, camphorsulfonate, citrate, digluconates, dodecylsulfates, ethanesulfonate, fumarate, gluconate, glutamate, glycerophosphates, hemisulfates, heptanoates, hexanoates, hydrobromides, hydrochloride, hydroiodides, 2-hydroxyethanesulfonates, isethionate, lactate, maleate, malate, mandelate, methanesulfonate, 2-naphthalenesulfonates, nicotinates, mucate, nitrate, oxalates, pectinates, persulfates, 3-phenylpropionates, picrates, pivalates, propionates, pamoate, pantothenate, phosphate, salicylates, succinate, sulfate, sulfonates, tartrate, p-toluenesulfonate, and the like.

Benzofuran derivatives which contain an acidic moiety, such as, but not limited to a carboxylic acid, may form salts with variety of organic and inorganic bases. Suitable pharmaceutically acceptable base addition salts for the compounds of the present invention include, but are not limited to, ammonium salts, metallic salts made from calcium, lithium, magnesium, potassium, sodium and zinc or organic salts made from lysine, N,N-dialkyl amino acid derivatives (e.g. N,N-dimethylglycine, piperidine-1-acetic acid and morpholine-4-acetic acid), N,N'-dibenzylethylenediamine, chloroprocaine, choline, diethanolamine, ethylenediamine, meglumine (N-methylglucamine), t-butylamine, dicyclohexylamine, hydrabamine, and procaine.

The benzofuran derivatives may exist in their tautomeric form (for example, as an amide or imino ether). All such tautomeric forms are contemplated herein as part of the present invention.

The compounds described herein may contain asymmetric centers and may thus give rise to enantiomers, diastereomers, and other stereoisomeric forms. Each chiral center may be defined, in terms of absolute stereochemistry, as (R)- or (S)-. The present invention is meant to include all such possible isomers, as well as, their racemic and optically pure forms. Optically active (R)- and (S)-, or (D)- and (L)- isomers may be prepared using chiral synthons or chiral reagents, or resolved using conventional techniques. When the compounds described herein contain olefinic double bonds or other centers of geometric asymmetry, and unless specified

otherwise, it is intended that the compounds include both E and Z geometric isomers.

Compositions and inhibitors of the present disclosure may also include a pharmaceutically acceptable carrier, in particular a carrier suitable for the intended mode of administration, or salts, buffers, or preservatives. Certain of the compounds disclosed herein are poorly soluble in water. Accordingly, aqueous compositions of the present disclosure may include solubility enhancers. Compositions for oral use may include components to enhance intestinal absorption. The overall formulation of the compositions and inhibitors may be based on the intended mode of administration. For instance, the composition may be formulated as a pill or capsule for oral ingestion. In other examples, the composition may be encapsulated, such as in a liposome or nanoparticle.

Compositions of the present disclosure may contain a sufficient amount of one or more inhibitors to cause inhibition of a bacterium (such as, for example, *Mtb*) to occur when the composition is administered to the bacterium. The amount can vary depending on other components of the composition and their effects on drug availability in a patient, the amount of otherwise required to inhibit the bacterium, the intended mode of administration, the intended schedule for administration, any drug toxicity concerns, drug-drug interactions, such as interactions with other medications used by the patient, or the individual response of a patient. Many compositions may contain an amount well below levels at which toxicity to the patient becomes a concern.

The amount of inhibitor present in a composition may be measured in any of a number of ways. The amount may, for example, express concentration or total amount. Concentration may be for example, weight/weight, weight/volume, moles/weight, or moles/volume. Total amount may be total weight, total volume, or total moles. Typically, the amount may be expressed in a manner standard for the type of formulation or dosing regimen used.

Methods of Bacterial Inhibition

The present disclosure also provides methods of inhibiting a bacterium with an inhibitor as disclosed. In certain embodiments in which a bacterium is inhibited by administration of an inhibitor, the dosage and administration may be adequate to allow this inhibition. In certain embodiments, it may consist of regular administration of an amount of the inhibitor, to maintain

a certain level of the inhibitory compound or compounds in the patient, the patient's blood, and/or a tissue in the patient. However, dosage amounts and the administration schedule may be adjusted based on other components of the composition and their effects on drug availability in a patient, the intended mode of administration, the intended schedule for administration, any toxicity concerns, and the patient's response to the inhibitor.

Without limiting the compositions and methods of administration described herein, in certain embodiments, the inhibitor can exhibit its inhibitory effect on a bacterium by directly or indirectly inhibiting fatty acid (e.g., mycolic acid) biosynthesis. In certain embodiments, this inhibition is mediated by binding of the inhibitor to a portion of a Pks13 enzyme in the bacterium. In certain embodiments, the portion of the Pks13 enzyme in the bacterium is the C-terminal thioesterase domain.

In certain embodiments, the inhibitors disclosed herein can be used for inhibition of a bacterium expressing Pks13. In certain embodiments of the present disclosure, the bacterium expressing Pks13 is a member of the suborder *Corynebacterineae*. In certain embodiments of the present disclosure, the bacterium expressing Pks13 is a *Mycobacterium*. In certain embodiments of the present disclosure, the bacterium expressing Pks13 is *Mycobacterium tuberculosis*. In certain embodiments of the present disclosure, the bacterium expressing Pks13 is *Mycobacterium leprae*. In certain embodiments of the present disclosure, the bacterium expressing Pks13 is *Corynebacterium diptheriae*. The bacterium can be located in any region of a patient, such as the lung. The bacterium may be latent or active.

In certain embodiments, the inhibitors disclosed herein can be used for inhibition of a bacterium expressing a close structural analog of Pks13. For example, in certain embodiments, the inhibitors disclosed herein can inhibit a bacterium expressing a close structural analog of Pks13 which is essential for the viability of the bacterium and contains a domain that is highly homologous to the Pks13 thioesterase domain.

The present disclosure is not limited by the precise target of inhibition. Inhibitors of the present disclosure can be used to inhibit any bacterium susceptible to inhibition by the inhibitor, irrespective of the precise mechanism of inhibition.

A bacterium present in a patient may be inhibited by delivering the inhibitor to the patient. The mode of delivery may be selected based on a number of factors, including

metabolism of the inhibitor, the mode of administration of other drugs to the patient, the location and type of bacterium to be inhibited, the health of the patient, ability or inability to use particular dosing forms or schedules with the patient, preferred dosing schedule, and ease of administration. In specific embodiments, the mode of administration may be enteral, such as orally or by introduction into a feeding tube. In other specific embodiments, the mode of administration may be parenteral, such as intravenously or by inhalation.

The dosage amounts and administration schedule of the inhibitor can vary depending on other components of the composition and their effects on drug availability in a patient, the severity of infection, the intended schedule for administration, any drug toxicity concerns, and the patient's response to the drug. In certain embodiments, the amount and frequency of delivery may be such that levels in the patient remain well below levels at which toxicity to the patient becomes a concern. However the amount and frequency may also be such that the levels of inhibitor in the bacterium temporarily reach or continuously remain at a level sufficient to cause inhibition of the bacterium.

In certain embodiments, the administration of the inhibitor is calibrated to reach a threshold concentration in the plasma or tissue of a patient. Such calibration can take into consideration experimentally derived bioavailability, such as the exemplary study data provided below, as well as the mass of the patient. In certain embodiments, the threshold concentration is a proportion of the minimum inhibitory concentration (MIC). Representative MIC data for representative inhibitors is provided above.

In certain embodiments, and based on one or more of the considerations discussed, the unit dosage of the inhibitor is between about 1 mg/kg body weight to about 500 mg/kg body weight. In certain embodiments, the unit dosage is between about 5 mg/kg to about 350 mg/kg. In certain embodiments, the unit dosage is between about 10 mg/kg and about 200 mg/kg body weight.

In certain embodiments, the inhibitor has an MIC value against *Mycobacterium tuberculosis* of about 0.1 μM to about 50 μM, or about 0.3 μM to about 20 μM, or about 0.35 μM to about 12.5 μM, or about 1 μM to about 10 μM, or about 1 μM to about 15 μM, or about 1 μM to about 25 μM. In certain embodiments, the inhibitor has an MIC against Mtb of less than about 5 μM, or less than about 3 μM, or less than about 1 μM.

The present disclosure further includes methods of identifying whether an inhibitor is able to inhibit a bacterium. Such methods include preparing or obtaining such a derivative, applying it to a bacterium, and identifying that the derivative inhibits the bacterium.

The present disclosure further includes methods and uses of the inhibitors for making and/or manufacturing drugs for inhibition of a bacterium, including, for example a bacterium expressing Pks13, an *Mtb* bacterium, and any other susceptible bacterium.

In certain embodiments of the disclosed subject matter, any of the inhibitors recited above are obtained by chemical synthesis.

In certain embodiments, an inhibitor is administered with one or more antibacterial, antibiotic and/or chemotherapeutic drugs. For example, the inhibitor can be administered with one or more antimycobacterial drugs, including one or more antitubercular drugs. In certain exemplary embodiments, an inhibitor is administered with one or more drugs selected from the group consisting of isoniazid, rifampicin, pyrazinamide, ethambutol, rifapentine, rifabutin. streptomycin, kanamycin, and amikacin, capreomycin, viomycin, ciprofloxacin, levofloxacin, moxifloxacin, ofloxacin, gatifloxacin, *para*-aminosalicylic acid, cycloserine, terizidone, ethionamide, prothionamide, thioacetazone, linezolid, clofazimine, amoxicillin, clavulanate, imipenem, cilastatin, and clarithromycin.

In certain embodiments, two or more inhibitors may be administered simultaneously or in sequence. The administration of two or more inhibitors may help prevent the development of resistance to one or more of the inhibitors.

In certain embodiments according to the disclosed subject matter, an inhibitor is simultaneously co-administered with one or more antibacterial or antibiotic drugs, such as one or more antitubercular drugs. In further embodiments, an inhibitor is administered prior to and concomitantly with administration of one or more antibacterial or antibiotic drugs, such as one or more antitubercular drugs. In still further embodiments, an inhibitor is administered prior to, concomitantly with, and after administration of one or more antibacterial or antibiotic drugs, such as one or more antitubercular drugs.

Any of the inhibitors may be administered in an amount and for a time sufficient to inhibit a Pks13 enzyme, and/or to improve the ability of one or more antibacterial or antibiotic drugs to kill a pathogen. Frequency of administration may be such that a selected minimum

amount of inhibitor remains biologically available at all times during the course of administration.

In certain embodiments in accordance with the disclosed subject matter, the inhibitors are administered orally (i.e. by enteral administration). Such oral administration can be by solid pill, liquid capsule, drink, nutritional supplement, meal, or any other means of oral administration. In alternative embodiments, the inhibitors are administered by parenteral administration, including, without limitation, intramuscular or subcutaneous injection and intravenous infusion.

Patients may include mammals, such as humans, pets, such as dogs and cats, and livestock, such as cattle, sheep, horses, and pigs. Patients may also include birds, such as chickens, turkeys, ducks, geese, quail and other poultry. Patients may be infected with a bacterium that is susceptible to an inhibitor according to the present disclosure, such as a bacterium expressing Pks13.

In a specific embodiment in accordance with the disclosed subject matter, a pharmaceutical composition may be formed containing an inhibitor as described above. The composition may contain additional compositions to stabilize or preserve the benzofuran derivative or derivatives. The composition may further contain compositions to increase uptake, particularly enteral uptake, or bioavailability of the inhibitor. Furthermore, the composition may contain other therapeutically active agents to be co-administered with the inhibitor or inhibitors, such as an additional antibacterial/antibiotic/antitubercular drug.

Benzofuran Derivatives for Pks13 Inhibition

Pks13 was previously identified as a viable target for tubercular inhibition. As early as 2004, Pks13 was shown to be essential to survival of mycobacterial species. Recently, and as described in Sacchettini *et al.*, *Identification of New Drug Targets and Resistance Mechanisms in Mycobacterium Tuberculosis*, PLOS ONE 8:9 (Sept. 2013), incorporated by reference herein in its entirety, a benzofuran-based compound ("the test compound") identified from a whole-cell screen was putatively found to target polyketide synthase Pks13, with an MIC of 2.0 μM against *Mtb* isolate H37Rv. The structure of the test compound is shown below.

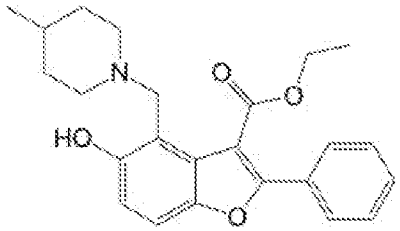

[Test Compound] (ID 1)

The same study further identified 7 additional compounds exhibiting whole-cell *Mtb* inhibition, each having a distinct target of inhibition. An additional *Mtb* Pks13 inhibitor was recently described based on a thiophene core with an alternative putative binding site (fatty-acyl-AMP loading at the N-terminal of Pks13). Although the test compound was shown in a high-throughput screen to have whole-cell antitubercular activity, and sequencing of resistant mutants suggested Pks13 to be its putative intracellular target, the present disclosure establishes for the first time that Pks13 is indeed the target of the test compound and additional compounds in this series.

Thus the present disclosure establishes that Pks13, an essential polyketide synthase from *Mtb,* is the target of novel benzofuran-based inhibitors, and further provides a novel genus of Pks13 inhibitors. Compounds in this series are shown to specifically bind to and inhibit the TE domain of Pks13. The present disclosure further provides the first disclosure of the structural basis of inhibition of Pks13. The consensus structure of the inhibitors is also disclosed, and key structural sites for inhibitor activity are identified. On the basis of this structure-activity analysis, Inhibitors having potency at least an order of magnitude greater than the test benzofuran derivative were identified.

The inhibitors were found to be generally non-cytotoxic to mammalian cells and shown to be effective inhibitors of *Mtb* in vivo. Certain inhibitors, however, did exhibit toxicity *in vitro* and *in vivo*. These and other aspects of the disclosure are discussed in detail below in the Examples that follow.

EXAMPLES

The following examples are provided to further illustrate certain embodiments of the disclosure. They are not intended to disclose or describe each and every aspect of the disclosure in complete detail and should be not be so interpreted. Unless otherwise specified, designations of cells lines and compositions are used consistently throughout these examples.

Pks13 Thioesterase Domain Enzyme Inhibition by Benzofuran Derivative

To confirm inhibitor activity against the TE domain of Pks13, recombinant expression constructs were generated encompassing different start and stop sites for the TE domain of *Mtb* Pks13 based on the sequence alignments and the secondary structure from homologs. One of the constructs encompassing the residues 1451-1733 of Pks13 expressed well in *E. coli* as His_6-tagged protein. This construct contained three additional residues at its N-terminus that were derived from the TEV cleavage site on the vector. The protein was soluble even after removal of the tag and produced single diffraction quality crystals. An enzyme assay for thioesterase activity was developed using this purified recombinant TE domain (hereafter called Pks13-TE), with the fluorescent substrate 4-methylumbelliferyl heptanoate (4-MUH). Pks13-TE showed good esterase activity using 4-MUH as the substrate with a $K_m \sim 20$ μM, and $k_{cat}/K_m \sim 7.2 \times 10^{-4}$ μM^{-1} min^{-1}.

The two mutant forms of the TE domain containing the resistance mutations from WGS (D1607N and D1644G) were also expressed and purified using an identical recombinant expression system as was used for the wild-type TE domain construct. As shown in Table 8, below, both mutants also exhibited thioesterase activity in the enzyme assay. Both mutations had an increased k_{cat}/K_m, with the D1607N mutant showing an increase of ~1.7-fold and the D1644G mutant >3-fold over the wt-Pks13-TE.

Table 8: Kinetic Parameters of Wild-Type Pks13-TE and D1607N, D1644G Pks13-TE Mutants

Protein	K_m (μM)*	k_{cat} min^{-1}	k_{cat}/K_m μM^{-1} min^{-1}	Relative activity
Wt.	19.5 ± 3.4	140 ± 9 $x10^{-4}$	7.2 ± 1.3 $x10^{-4}$	1
D1607N	8.5 ± 0.9	105 ± 3 $x10^{-4}$	12.3 ± 1.4 $x10^{-4}$	1.7
D1644G	6.9 ± 1.1	166 ± 6 $x10^{-4}$	24 ± 3.8 $x10^{-4}$	3.3

*Kinetics values were obtained by fitting the raw data to the Michaelis-Menten equation. All assays were carried out in triplicate. Results are presented as mean ± s.d.

The IC_{50} of the test compound against Pks13-TE was determined to be 0.26 μM. The D1644G mutation increased the IC_{50} of the test compound by more than 66-fold from 0.26 μM to 17.4 μM against the TE domain, and approximately 3-fold (to ~0.76 μM) for the D1607N mutant.

Crystal Structure of Apo Pks13-TE and Pks13-TE in Complex with Test Compound

To determine the molecular basis of the inhibition of Pks13-TE observed with the test compound, the crystal structure of Pks13-TE in complex with the test compound was solved. To first solve the apo-structure, thin, plate-like crystals of apo-Pks13-TE were obtained by vapor-diffusion method in a condition with ammonium sulfate as the precipitant at pH 8.5. The crystals diffracted to a maximum resolution of 1.7 Å, and they belonged to the space group $P2_12_12$ with two molecules in the asymmetric unit (designated *A* and *B*). The phase solution for the apo-Pks13-TE structure was determined by the molecular replacement method, using the crystal structure of *E. coli* EntF (PDB code 3TEJ) as the search model. The final apo-structure contained two molecules, *A* and *B*, with 278 and 272 residues built out of 283 residues, respectively, and was refined to a resolution of 1.72 Å (R_{work} = 17% and R_{free} = 20%) with good stereochemistry. The apo, test compound-bound, and D1607N mutant Pks13-TE crystal structure modeling data are shown in Table 9 below.

Table 9 - PKS13-TE Structure Refinement Data

	Apo Pks13-TE	Pks13-TE:**test**	Pks13-TE(D1607N)
Data collection			
Space group	$P2_12_12$	$P2_12_12$	$P2_12_12$
Cell dimensions			
a, *b*, *c* (Å)	88.5, 106.7, 57.7	89.2, 109.5, 57	88.7, 108.9, 58.1
α, β, γ (°)	90, 90, 90	90, 90, 90	90, 90, 90
Resolution (Å)	39.19-1.72 (1.75-1.72)*	39.5-1.94 (1.97-1.94)	44.36-1.88 (1.91-1.88)
R_{merge}	0.089 (0.55)	0.172	0.141
$I / \sigma I$	23.81 (4.33)	18.8 (2.3)	8.64 (0.53)
Completeness (%)	99.8 (96.1)	94.1 (93.29)	92.5 (59.1)
Redundancy	7.7 (6.7)	6.6 (5.2)	4.9 (2.6)
Refinement			
Resolution (Å)	1.72	1.94	1.88
No. reflections	58442	39903	42945
R_{work} / R_{free}	0.172/0.201	0.191/0.235	0.182/0.222
No. atoms			
Protein	4278	4218	4258
Ligand/ion	27	63	44
Water	387	206	293
B-factors			
Protein	22	47	35
Ligand/ion	31	48	54
Water	28	45	40

R.m.s. deviations			
Bond lengths (Å)	0.011	0.007	0.014
Bond angles (°)	1.35	1.19	1.44

*Values in parentheses are for highest-resolution shell. Data from 1 crystal was used to solve each structure.

As shown in FIG. 1, the Pks13-TE structure is divided into two domains (lid and core), with the larger core domain (residues 1451-1570, 1646-1660 and 1680-1733) possessing a canonical α/β-hydrolase fold comprised of a central seven-stranded β-sheet (β1- β7) flanked by four α-helices (α1-α3 and α11) with the N-terminal β1 strand anti-parallel to other strands. The smaller lid domain (residues 1575-1645) is inserted between strands β5 and β6 of the core domain and consists of four α helices, α4-α7, adjacent to the core domain. Two small helices, α8 and α9, (residues 1665-1675) that are present on a long loop between strands β6 and β7 of the core domain also form part of the lid domain. The topology of the TE domain in the Pks13-TE-test compound complex structure is very similar to the apo-enzyme structure (RMSD of 0.94 Å over 272 paired C_α atoms).

Analysis of the TE1451 structure with VAST server uncovered >100 structures belonging to thioesterase, hydrolase and lipase class enzymes with structural alignment scores well above the threshold of significance (VAST -log(p)>10). The top hit (VAST -log(p)>15) in the structural alignment was the thioesterase of fengycin synthesis, a non-ribosomal peptide synthetase (PDB code 2CB9) from *B. subtilis*. However, regardless of the enzyme class, the structural similarity was within the α/β-hydrolase core domain; the lid domain did not show significant structural conservation among the hits. In a VAST search using only the coordinates of the lid domain (1575-1645), only three hits were returned with alignment scores well below the significance threshold (VAST -log(p)<4) which had no structural or functional relationship with the lid domain. This finding is consistent with the role of lid domains in substrate recognition and binding in a variety of α/β-hydrolase enzymes, which accounts for their highly variable substrate specificities.

The active site of Pks13-TE was identified as a canonical Ser-His-Asp catalytic triad, similar to other α/β-hydrolase thioesterases. By superimposition of the Pks13-TE structure on the *E. coli* EntF structure (PDB code 3TEJ) as shown in FIG. 2, Ser1533 was identified as the active site nucleophile, and Asp1560 and His1699 as the other two members of the catalytic triad. The active site pocket is formed at the interface between the two domains, and it is

situated at the proximal end of a long surface groove in the lid domain. This groove spans the full length of the lid domain (~30 Å) with a total surface area ~1290 $Å^2$, as calculated using the CASTp server. The active site of the Pks13-TE domain is shown in FIG. 3. The residues lining this groove are primarily hydrophobic, suggesting it could bind long-chain fatty acid substrates. A similar hydrophobic surface groove (~ 20 Å long) leading to the active site serine was also observed in the α-helical lid domain of bovine palmitoyl-protein thioesterase 1 bound to palmitate. Additionally, a fragment of polypropylene glycol ($C_{12}O_5H_{25}$), an additive in the crystallization buffer, was observed bound in the active site of the apo-TE domain structure. Thus, the structure strongly suggests that the surface groove presents the substrate-binding site that can accommodate the meromycolate product and position it for de-esterification by the catalytic triad.

Next, crystals of Pks13-TE complexed to the test compound were obtained by soaking the apo-Pks13-TE crystals with the test compound. The complex structure was determined by molecular replacement to a resolution of 1.94 Å (space group $P2_12_12$ and unit cell similar to apo-Pks13-TE) with 273 and 274 residues built out of a total of 283 residues for molecules A and B, respectively, and refined to a final R_{work} = 19% and R_{free} = 23%. The test compound-bound Pks13-TE crystal structure data are also provided in Table 9 above.

As shown in FIG. 3, the test compound binds at the mouth of the substrate-binding groove, approximately 6Å from the catalytic site. Binding of the inhibitor thus effectively blocks access of the substrate to the active site. The four different substituents attached to the benzofuran scaffold interact mainly with the residues from helix α7 of the lid domain (Gln1633, Ser1636, Tyr1637, Asn1640, Arg1641, Ile1643 and Asp1644) and the two supporting helices α8-α9 along with the loop that connects them to strand β6 of the core domain (Tyr1663, Ala1667, Phe1670, Glu1671 and Tyr1674). These binding interactions are summarized in Table 10 below

.

Table 10: Interactions of Test Compound with Pks13-TE Domain Residues

TE domain residue	**Type of interaction**	**Interacting group**
Phe1670	Planar stacking, hydrophobic	Benzofuran core
Asp1644	Hydrogen bond (2.4 Å)	-OH at C-5

Asn1640	Hydrogen bond (3 Å)	Basic N of piperidine at C-4
Gln1633, Ser1636	van der Waals	Phenyl at C-2
Tyr 1674, Tyr1663, Ala1667	van der Waals	Piperidine ring at C-4
Glu1671	van der Waals	-OH at C-5
Tyr1582, Tyr1637	van der Waals	Phenyl ring of core
Arg1641, Ile1643	Hydrophobic	Phenyl ring of core and methyl of piperidine

Several changes occur upon binding of the test compound, as depicted in FIG. 4. Most notably, Phe1670, located at the end of helix α8, flips to form a planar stacking interaction (3.6-3.7 Å) with the furan ring of the benzofuran and hydrophobic interactions with the phenyl component of the fused-ring system. The Phe1670 side chain also forms van der Waals interactions with the phenyl ring and the ethyl group of the ethyl ester attached to the test compound, respectively (~4 Å).

The side chains of Tyr1582 and Tyr1637 also participate in van der Waals interactions with the phenyl ring of the benzofuran core (3.7-3.8 Å). One of the key interactions for binding of the test compound involves Asp1644, which is located at the end of helix α7 of the lid domain. The carbonyl oxygen of Asp1644 forms a strong hydrogen bond (2.4 Å) with the hydroxyl of the benzofuran compound. In addition to the direct interactions with the benzofuran, a carboxylate oxygen at Asp1644 also forms a hydrogen bond with the hydroxyl of Tyr1674 (2.7 Å), helping to orient it to form a face-on van der Waals interaction with the piperidine ring. The basic nitrogen of the piperidine ring acts as a bifurcated donor, making one hydrogen bond with the side chain oxygen of Asn1640 (3 Å) and another with the carbonyl oxygen of the ethyl ester (3.3 Å). Other residues that participate in the van der Waals interactions with the test compound are Gln1633 and Ser1636, with the phenyl ring; Tyr1663 and Ala1667, with the piperidine; and Glu1671, with the hydroxyl. Arg1641 and Ile1643 form hydrophobic interactions with the phenyl ring of the benzofuran core and the methyl group of the piperidine, respectively.

Thus the benzofuran binds non-covalently in a hydrophobic cleft between the core α/β-hydrolase and helical-lid domains, at the entrance of the catalytic chamber of the TE domain.

This establishes the mechanism of inhibition, as it effectively blocks access of the meromycolate substrate to the active site Ser1533. In contrast, inhibitors of the human FAS TE domain were previously reported to exert their inhibitory effects by forming a covalent adduct that mimics the acyl-enzyme intermediate.

Structure-Activity Relationship and Potency Enhancement of Benzofuran Derivatives

To establish that compounds similar to the test compound also exhibit inhibition, and to develop a structure-activity relationship (SAR) for this series, second-generation structural analogs of the test compound were evaluated for inhibition of Pks13-TE activity *in vitro*. The analogs were selected and evaluated to test the effects of chemical modifications at each of the four substituent positions of the benzofuran scaffold as shown below.

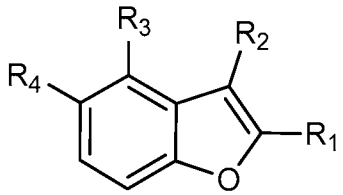

These compounds are shown in Table 11 below with their observed pharmacokinetics against Pks13-TE

Table 11 - Second-Generation Inhibitors for Structure-Activity Relationship Analysis

ID	R_1	R_2	R_3	R_4	IC_{50} (μM)*	MIC (μM)*
1		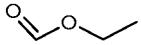	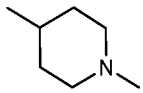	OH	0.26 ± 0.03	2.3 ± 0.2
2		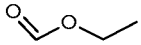	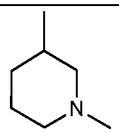	OH	0.12 ± 0.02	4.4 ± 0.2
3		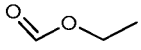	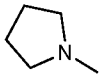	OH	0.24 ± 0.02	4.1 ± 0.1
4		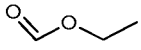	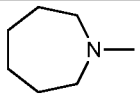	OH	0.28 ± 0.03	4.6 ± 0.3
5		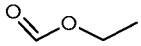	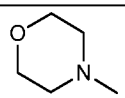	OH	0.71 ± 0.05	13.3 ± 1.6

109		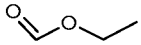		OH	1.57 ± 0.15	7.3 ± 0.3
6		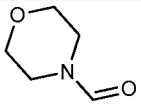	H	OH	No binding	ND
7		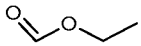	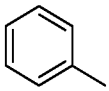	OH	11.9 ± 2.3	>40
13		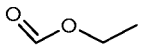	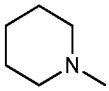	OH	0.26 ± 0.04	0.4
14		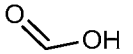	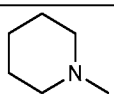	OH	6.6 ± 0.7	NI
16		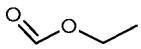	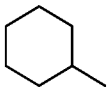	OH	19.6 ± 1.4	5.2
17		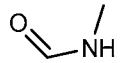	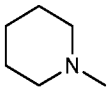	OH	0.29 ± 0.01	0.2
22	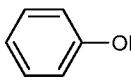	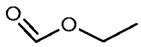	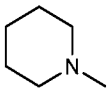	OH	0.17 ± 0.02	1.2
23		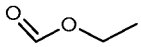	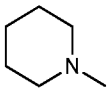	MeO	35.8 ± 2.2	ND
24		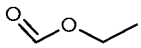	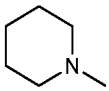	H	2.0 ± 0.1	16

*Values are shown as mean ± s.d. of triplicates. MeO: methoxy; ND: not determined; NI: no inhibition.

IC_{50} values were determined using the *Mtb* Pks13-TE domain as described in the methods section below. MIC values were determined for *mc*^{2}7000 *Mtb* isolates in liquid medium in 96-well plates.

The SAR studies for the R_3 position were designed to investigate the effect of ring planarity and the role of the N-atom in inhibitor potency. On the basis of the Pks13-TE-test compound complex structure, it was hypothesized that the puckered piperidine might be replaceable by a phenyl ring, which could π-stack with Tyr1674. However, neither compound H having a phenyl group nor compound K having a puckered cyclohexyl group showed significant enzyme inhibition activity, exhibiting a loss of activity by >40- and >70-fold respectively, when compared to the test benzofuran compound. It was found that other saturated heterocycles (compounds B-E) maintained activity. The IC_{50} values ranged from 0.12 – 1.57 μM against the TE domain). IC_{50} data shows that compound B was more potent (0.12 μM) compared to the test

compound (0.26 μM) against Pks13-TE. The only difference between these two positional isomeric compounds is that the methyl group on the piperidine ring is in *para* position in the test compound and in *meta* position in B. When the piperidine ring was replaced in the des-methyl analog I, it showed an IC_{50} (0.3 μM) similar to the test compound. Compounds C and D have five- and seven-membered rings, respectively, at R_3, and exhibited IC_{50} values similar to the test compound, whereas compound E, which has a six-membered morpholine ring with a polar oxygen atom, has ~3-fold higher IC_{50} against Pks13-TE compared to the test compound. In contrast to the compounds with cyclic amine substituents at R_3, compound F (having acyclic dimethyl amine at R_3) exhibited >6-fold loss in inhibitory activity relative to the test compound. In comparison, compound G, which lacks a substitution at R_3 altogether and has a morpholine ring at R_2 in place of the ethyl ester, did not show any appreciable binding to Pks13-TE, even at a concentration of 30 μM.

The structural basis for the inhibition of Pks13-TE by analogs of the test compound with replacement heterocycles at R_3 was determined by solving crystal structures of inhibitor complexes. The structures of Pks13-TE-analog binary complexes were refined using the Pks13-TE-apo structure. There was a clear positive $|F_o|-|F_c|$ difference electron density for inhibitors C-F, which were in a very similar position in the substrate-binding groove. Ligands were fit into the electron density, and the structures were built and refined to a resolution of 2 Å with good stereochemistry. These structures are shown in FIG. 4. The protein components of all the complexes exhibit a nearly identical overall structure as compared to the Pks13-TE-test compound complex (RMSD of 0.4 Å for compound D, 0.7 Å for compound C, and 0.9 Å for compounds E and F vs. test compound complex over 264 paired C_α atoms). In the structures, the variation in the tertiary amine group at R_3 of the second-generation analogs did not affect their mode of binding. Crystal structure data and refinement statistics for inhibitors C-F in complex with Pks13-TE are provided in Table 12 below.

Table 12 - Pks13-TE - Inhibitor Crystal Structure Data and Refinement Statistics

	Pks13-TE:**3**	Pks13-TE:**4**	Pks13-TE:**5**	Pks13-TE:**6**
Data collection				
Space group	$P2_12_12$	$P2_12_12$	$P2_12_12$	$P2_12_12$
Cell dimensions				
a, *b*, *c* (Å)	89.4, 109.4, 56.9	89, 110.2, 57.5	88.9, 109.7, 57.4	88, 109.4, 57
α, β, γ (°)	90, 90, 90	90, 90, 90	90, 90, 90	90, 90, 90

Resolution (Å)	33.76-1.99 (2.02-1.99)*	48.33-2.04 (2.12-2.04)	48.2-2.05 (2.10-2.05)	46.45-1.99 (2.04-1.99)
R_{merge}	0.114	0.158	0.158	0.124
$I / \sigma I$	14.1 (1.5)	9.0 (0.8)	11.5 (1.6)	9.9 (1.3)
Completeness (%)	87.8 (84.4)	87.6 (69.7)	94.0 (91.6)	99.0 (91.6)
Redundancy	5.2 (4.5)	4.3 (3.7)	5.5 (4.6)	4.3 (4.1)
Refinement				
Resolution (Å)	1.99	2.04	2.05	1.99
No. reflections	34374	32129	33649	38083
R_{work} / R_{free}	0.196/0.24	0.208/0.238	0.201/0.237	0.187/0.215
No. atoms				
Protein	4220	4239	4204	4236
Ligand/ion	54	34	28	50
Water	152	99	208	386
B-factors				
Protein	44	56	34	34
Ligand/ion	33	79	33	29
Water	45	53	34	38
R.m.s. deviations				
Bond lengths (Å)	0.009	0.005	0.007	0.008
Bond angles (°)	1.28	0.98	1.10	1.14

Binding of the test compound and compounds C-F to the Pks13-TE domain is illustrated in FIG. 5. The crystal structures revealed that the different cyclic amine groups at the R_3 position formed stacking interactions with Tyr1674 in a manner similar to the test compound. The small differences in the IC_{50} values between the test compound and compounds C and D can be attributed to variations in the strength of the stacking interactions of the planar side chain of Tyr1674 with the variably puckered rings at R_3, similar to the sugar-ring Tyr interactions in the carbohydrate/sugar binding proteins. In the Pks13-TE-E complex structure, it was observed that the polar cyclic amine at R_3 also stacked with Tyr1674; however, it formed only van der Waals interactions with side chains of Ile1643 and Tyr1663 (4-4.3 Å). Contrary to expectations, the oxygen atom of the R_3 morpholine ring of compound E did not form a hydrogen bond interaction with the hydroxyl of Tyr1663, as its rotamer conformation positioned the hydroxyl at a distance of 4.2 Å. The effect of the reduced interactions of compound E on its inhibitory activity was reflected in a ~3-fold increase in its IC_{50} (0.71 μM) compared to the test compound (IC_{50} 0.26 μM). In contrast to the cyclic groups at R_3, the presence of an acyclic dimethyl amine group at R_3 in compound F was expected to abolish the stabilizing stacking interaction with Tyr1674, and it was confirmed in the Pks13-TE-F complex structure. The structure also revealed that the smaller size of the side group at R_3 led to reduced van der Waals and hydrophobic interactions

with Tyr1674, Tyr 1663 and Ile1643. As a consequence of this loss of interactions, there was >6-fold decrease in the inhibitory activity of F against Pks13-TE.

Since the ethyl ester at position R_2 can be hydrolyzed to the corresponding acid by broad-specificity esterases inside *Mtb*, it is plausible that the carboxylic acid form of test compound is the active compound. This hypothesis was tested by synthesizing compound J, the acid analog of compound I. Compound J had an IC_{50} of 6.6 μM, a ~20-fold loss in activity compared to the ester-containing analog compound I. The ethyl ester represents a pharmacological liability, however, as it could also be subject to hydrolysis by serum esterases, leading to the production of the less-active acid form of the inhibitor. Thus compound L, a methyl-amide analog of compound I, was synthesized. Compound L showed similar enzyme inhibitory activity (IC_{50} 0.3 μM) as the ethyl ester-containing compound I and the test compound. Thus, the replacement of the ethyl ester at the R_2 position with an amide group maintained the inhibitor potency, while conferring to it the desired metabolic stability.

Testing of different substituents at the R_4 position demonstrated that the phenolic OH is important for inhibitor binding. This hydroxyl group forms a strong hydrogen bond with Asp1644, and hence is expected to contribute significantly to affinity. Two analogs of compound I were synthesized in which the R_4 OH was substituted with either a methoxy group (compound N) or a hydrogen atom (compound O). The IC_{50} for compound N was determined to be ~36 μM, whereas it was 2 μM for compound O. Thus, introduction of a bulkier group and the removal of hydrogen bonding capability in compound N caused a >100-fold decrease in its inhibitory activity, while compound O showed ~7-fold decrease in activity due to substitution of the R_4 OH with a hydrogen atom. It is possible that other hydrogen-bond donating groups at this or the adjacent position on the benzofuran ring could also yield inhibitors with high affinity.

The structure of the Pks13-TE complex with the test compound indicated that the side-chain amide of Gln1633 on helix α7 is positioned at a distance of ~4 Å from the distal end of the R_1 phenyl ring. On the basis of this observation, compound M was synthesized containing an OH group at the C-4 of the R_1 phenyl ring, to determine if the modification resulted in additional hydrogen bond interactions. Compound M exhibited a slightly better IC_{50} (0.19 μM) compared to the non-OH substituted compound I (IC_{50}: 0.3 μM). Thus, the hydroxylation of the R_1 phenyl ring at the para- position increases potency.

Whole-Cell Activity of Benzofuran Derivative Inhibitors Against Mtb

Whole-cell assays show that the ester-analogs of the test compound, but not the corresponding acids, have *Mtb* growth-inhibition activity. The analogs were tested for anti-*Mtb* activity in a whole-cell growth inhibition assay using the *Mtb* strain $mc^2$7000. All compounds that were active against Pks13-TE *in vitro* also inhibited the growth of *Mtb* bacteria to varying extents. Compounds B, C, and D had IC_{50} values comparable to the test compound against Pks13-TE, but they exhibited ~2-fold higher MICs against the bacteria. In comparison, compound E and F exhibited 6- and 3-fold higher MICs compared to the test compound. Notably, compound E had an IC_{50} value >2-fold lower than compound F against Pks13-TE *in vitro*, but in whole cell testing its MIC was ~2-fold higher than compound F. Since compound E is more polar, it is possible that this compound had reduced cell penetration, which subsequently resulted in an increase in its MIC. However, other effects like efflux or metabolism of compound E that can lead to an increase in its MIC cannot be ruled out. Among the synthesized analogs of the test compound, the whole-cell activity was completely abolished for the acid functionality containing analog J. When compound L was tested for the whole-cell activity, the MIC (0.2 μM) was found to be >10-fold lower than that of the test compound, suggesting that the replacement of the more labile ethyl-ester with the more stable amide group at the R_2 position significantly improved its whole-cell activity.

Experimental data indicated that compounds in this benzofuran series are not cytotoxic to human fibroblast cells. To assess the potential of the test compound and analogs that demonstrate good whole-cell activity (compounds B-E, I and L) as suitable candidates for further development, they were tested for cytotoxicity against human dermal fibroblast (HDF) cells using the resazurin dye assay. As shown in FIG. 6, the test compound and compounds B, D, E, I and L did not show any growth inhibition (relative to DMSO only control) in HDF cells up to 40 μM, whereas compound C exhibited a half-maximum inhibitory concentration of >15 μM. The low cytotoxicity suggests that these compounds have good selectivity *in vivo*.

Structural Basis for Distinct Mechanisms of Resistance in D1607N and D1644G Mutants

Crystal structures of the mutant proteins containing the resistance mutations identified by WGS suggest that they cause resistance to the test compound and its analogs through different mechanisms. The effect of D1644G mutation is direct, in that it removes the interaction with the R_4 hydroxyl of the test compound. The effect of the D1607N mutation is less apparent because it does not make any direct interactions with the test compound. Inspection of the interactions of Asp1607 in the D1607N mutant structure revealed that in the wtPks13-TE-test compound complex structure the side chain carbonyl oxygen atoms of Asp1607 form bidentate hydrogen bond interactions with the side chain amine group of Arg1641 (3.1 Å) which helps to anchor the C-terminal end of the α7 helix in a position that facilitates Asp1644 to form hydrogen bond interaction with the R_4 hydroxyl of the test compound and with Tyr1674. In contrast, and as shown in FIG. 7, the D1607N mutation disrupts this hydrogen bond interaction with Arg1641, allowing it to adopt a different rotamer conformation. This results in the loss of the anchoring effect by Arg1641 and causes the C-terminal end of helix α7 to move away from the substrate-binding groove. The resulting flexibility also causes Asp1644 to move away from the substrate-binding groove by 3 Å, altering its hydrogen bond interactions. The movement of Asp1644 disrupts its interaction with the test compound; however, it still is positioned within hydrogen bonding distance to Arg1641 (2.7 Å). Thus, the D1607N mutation introduces subtle changes in structural interactions, in contrast to the D1644G mutation, to disrupt TE domain interaction with the test compound and impart resistance to the bacterium.

In vitro Mtb Cytotoxicity of Second- and Third-Generation Inhibitors

Based on the detailed SAR analysis discussed above, a third generation of representative benzofuran derivatives were synthesized. Pks13 enzyme inhibition of these inhibitors was tested as described herein. The structures and Pks13 enzyme inhibition data (MIC and IC_{50}) for representative inhibitors (test, second-, and third-generation) is provided in Tables 1-7 above.

Representative second- and third-generation inhibitors exhibiting potent Pks13 enzyme inhibition were further evaluated for whole cell inhibitory activity (cytotoxicity) against *mc*^{2}7000 *Mtb* isolate cells. The structures of the representative inhibitors are provided with corresponding pharmacokinetic data in Table 13 below. The Non-Toxic Concentration data represent the highest concentrations of the test compounds exhibiting little or no cytotoxicity to human dermal

fibroblast (HDF) cells, and the Survival vs. Control data represent percent survival of HDF cells relative to DMSO-only control. Where two values are provided, the first and second values in the Survival vs. Control column respectively correspond to percent HDF cell survival observed relative to DMSO-only control for the first and second values provided in the Non-Toxic Concentration column for the same compound.

Table 13: Representative high-potency inhibitor structure and pharmacokinetics

ID	Structure	Pks13 MIC (μM)	Pks13 IC_{50} (μM)	Non-Toxic Concentration (μM)	Survival vs. Control (%)
8	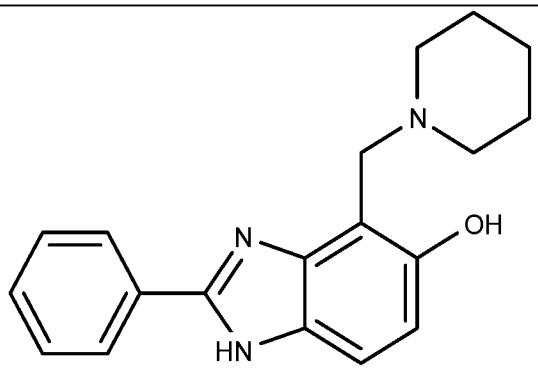	22	6.8	50, 25	78, 94
13	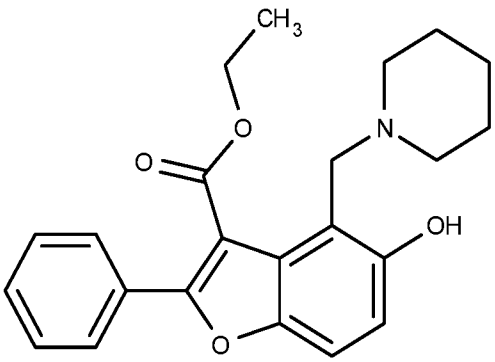	0.4	0.26	50	105
17	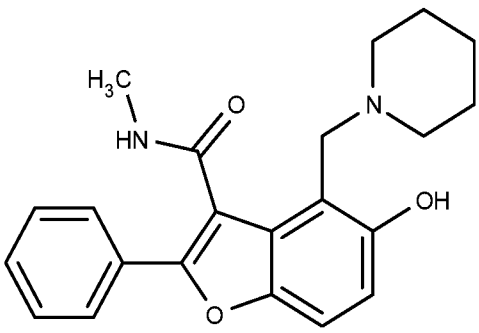	0.2	0.29	50	103

21	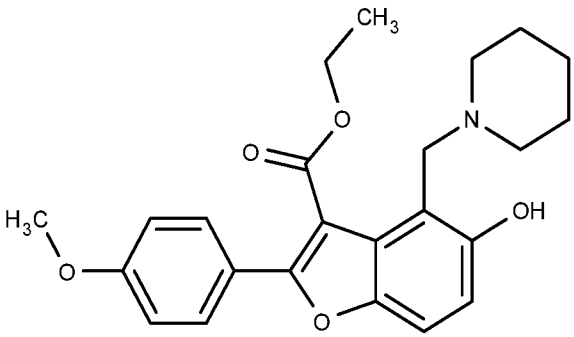	2.6	0.29	50	104
22	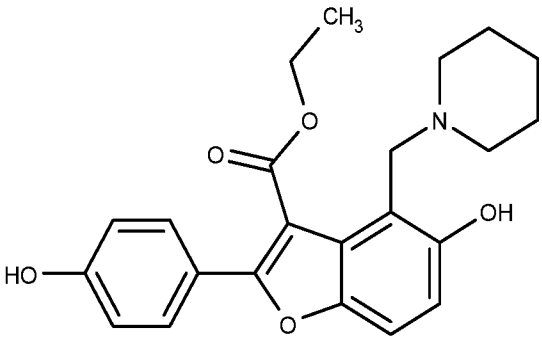	0.6	0.19	50	103
27	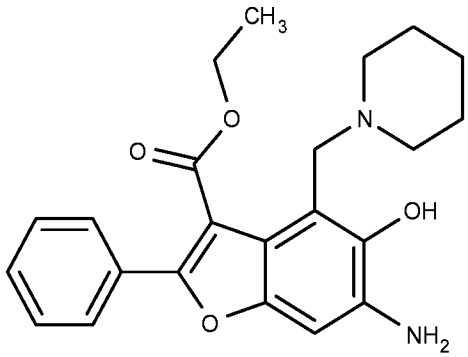	8	0.37	50, 25	77, 114
29	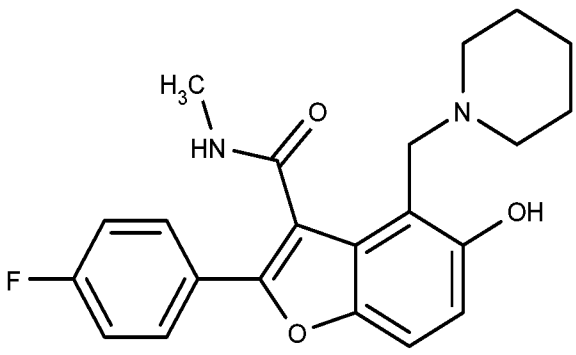	4.5	0.3	100, 50	89, 112

31	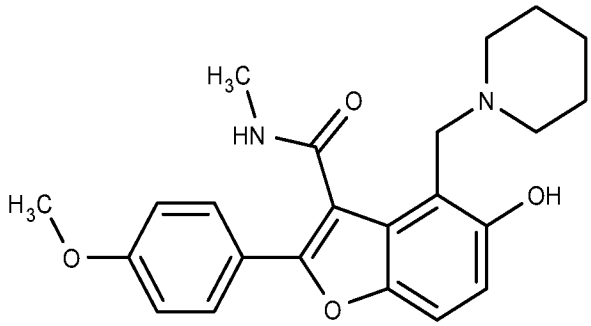	1.1	0.26	50	111
32	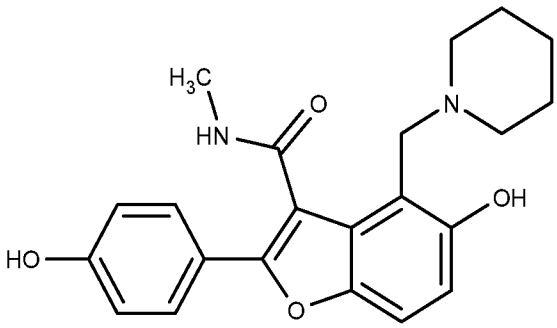	0.09	0.26	50	82
34	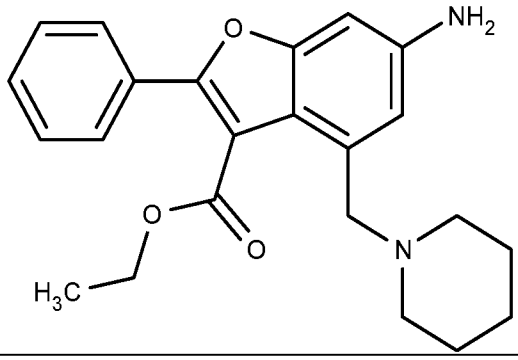	9.2	4.5	100	82
38	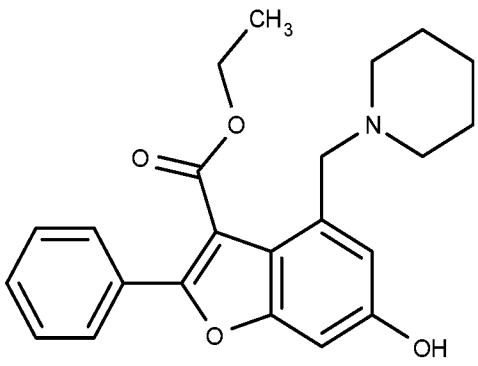	6.7	0.45	100	111

39	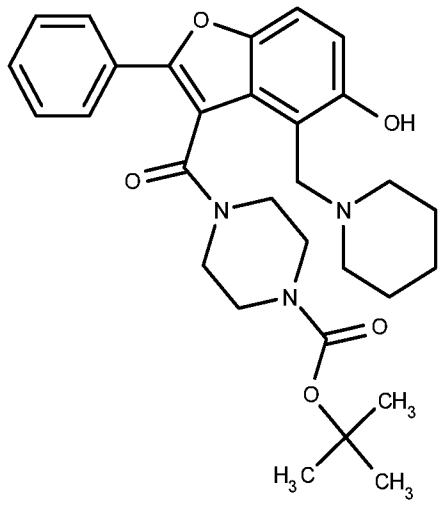	2.1	0.66	100	101
40	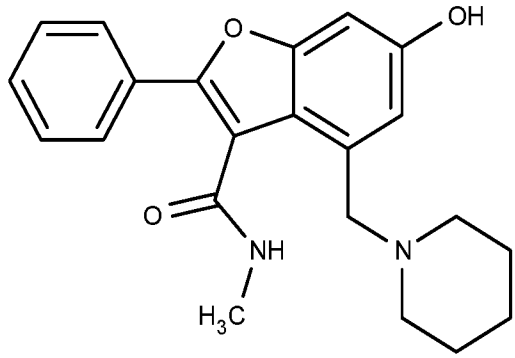	20	0.6	100	101
42	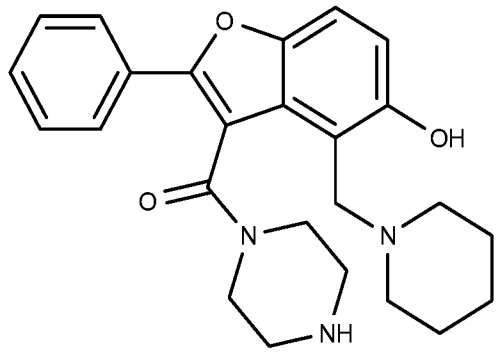	3.1	0.74	100	100
43	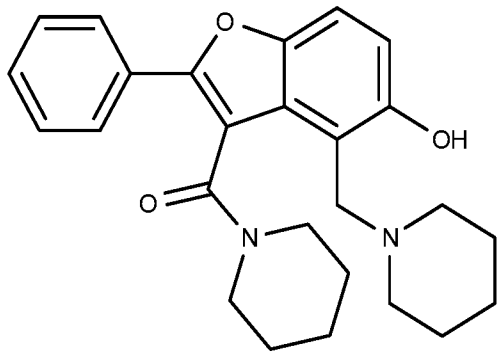	> 10	0.32	100	89

44	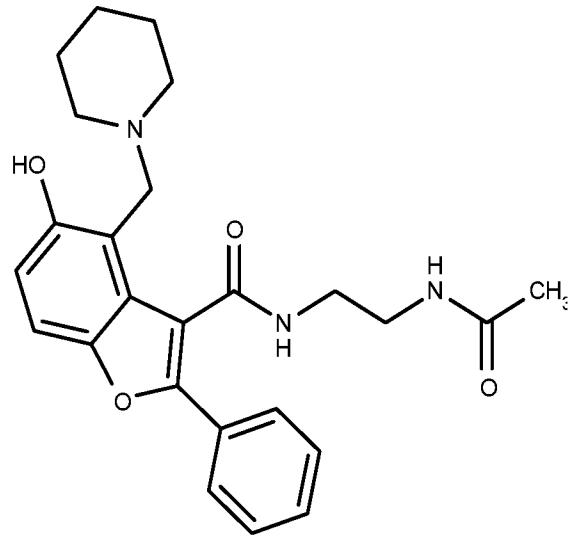	> 40	0.5	50	104
45	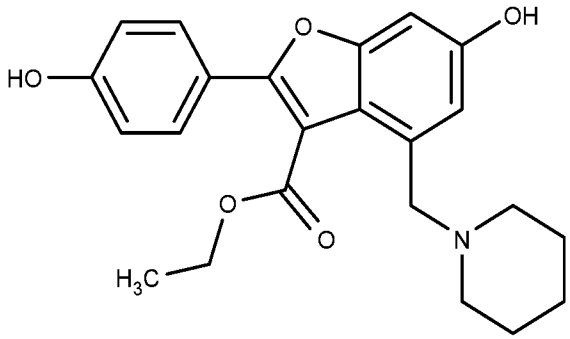	1.1	0.44	100	89
47	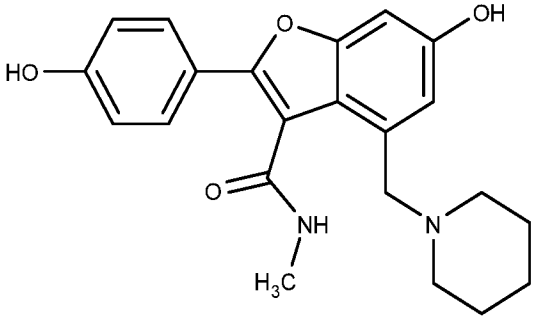	1	0.57	50	98

58	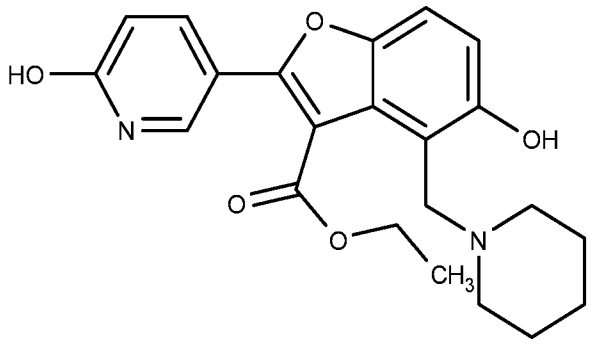	4	0.36	50	95
61	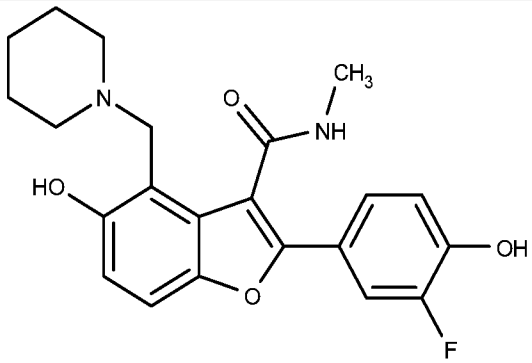	0.5	0.33	50	94
62	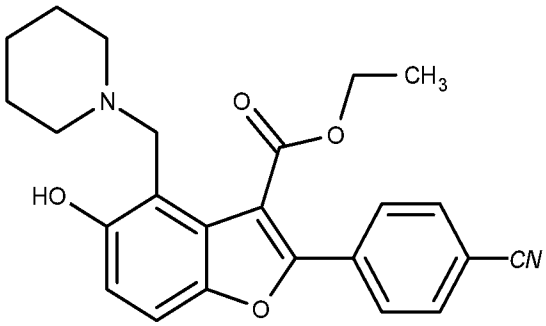	1.5	0.27	6.25	90
63	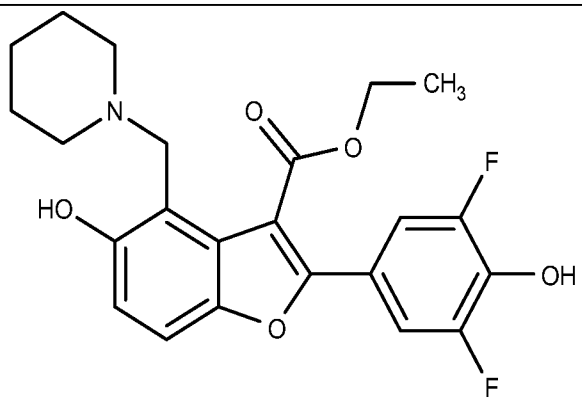	7	0.5	25	99

64	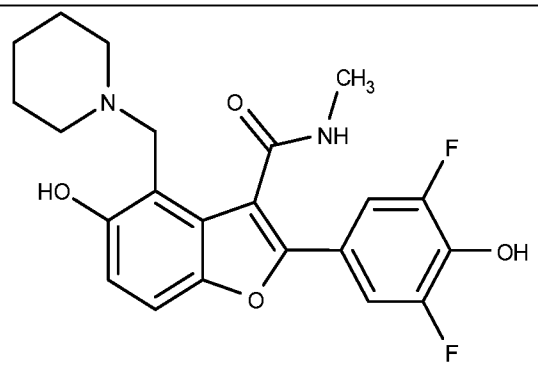	NI (40 μM)	1.5-1.9	100	94
65	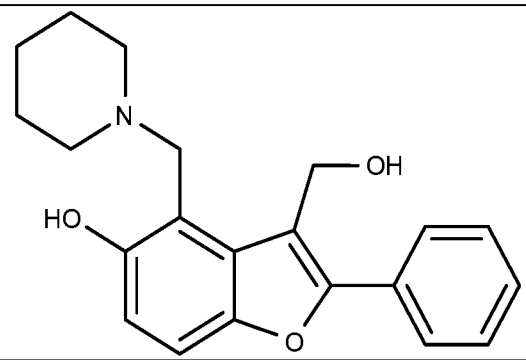	6 -12.5	0.24	25	95
67	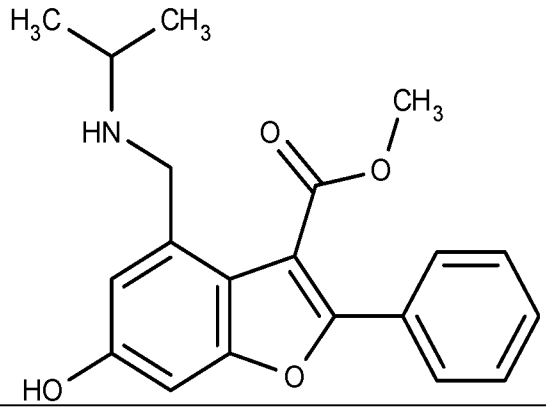	9	0.7	25	97
69	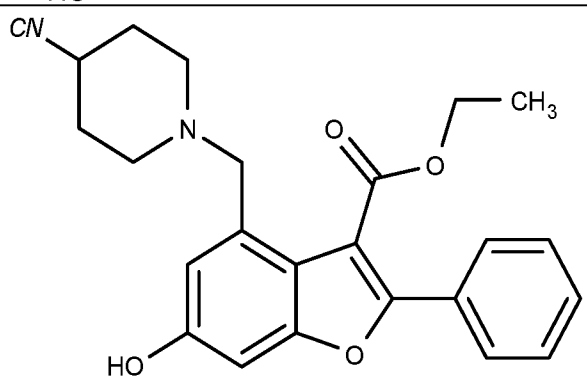	20	1.6	50	93

70	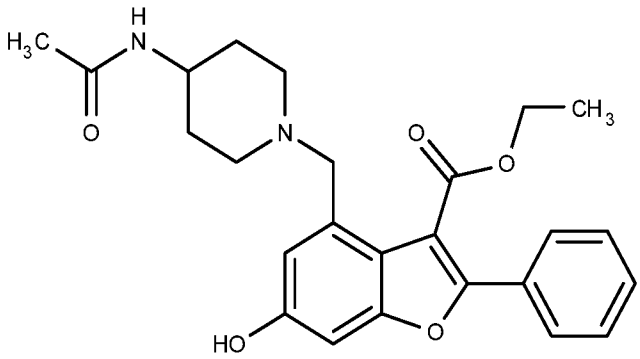	>40	6.1	50	91
72	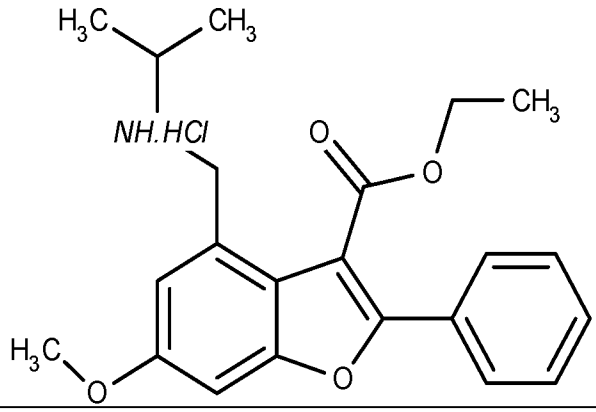	7.4	>10	3.125	91
73	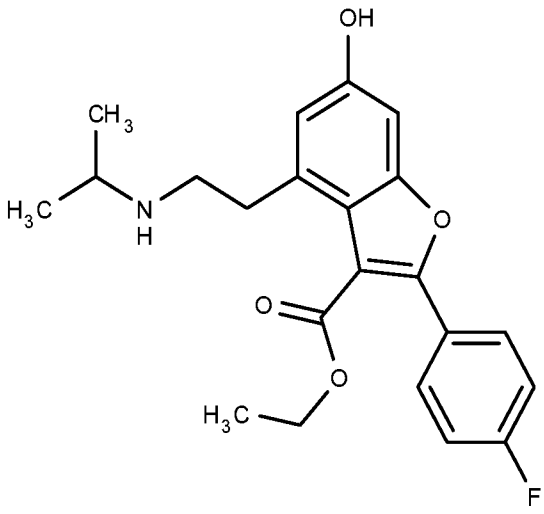	2.5	1.5-2.1	12.5	97

74	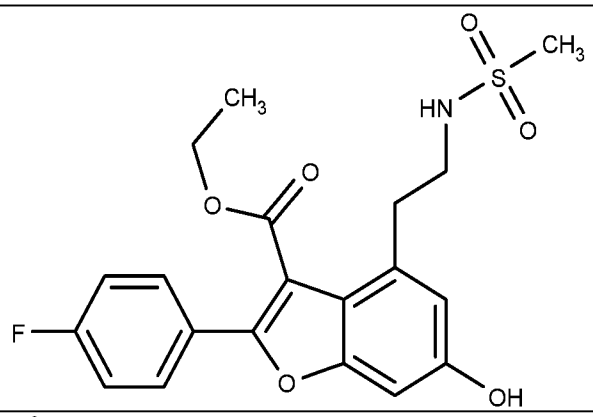		20	25	88
88	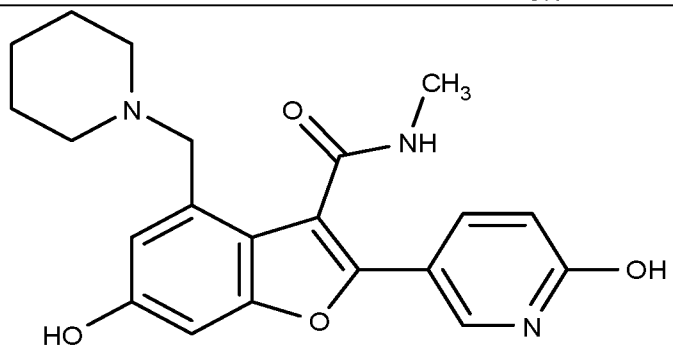		2.8	50	96
102	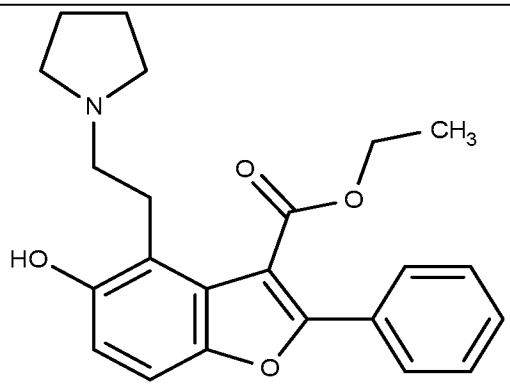		0.7	1.56	91
103	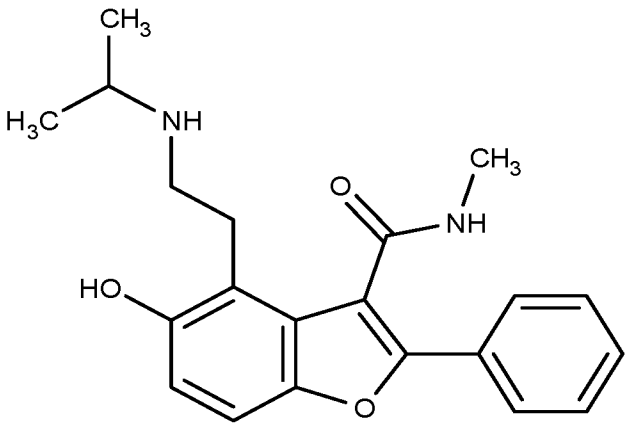		0.45	50	82

Efficacy Against Drug Resistant Mtb *Strains*

The efficacy of Inhibitor 32 against drug resistant *Mtb* strains was tested.. A non-drug resistant control strain, H37Rv, was tested as well. MDR strains are resistant to both isoniazid (INH) and rifampicin (RMP) and may also be resistant to other drugs. XRD strains were MDR strains that are also resistant to any fluoroquinolone, and to any of the three second-line injectables (amikacin, capreomycin, and kanamycin). Pre-XRD strains are MDR strains with additional resistance either a fluoroquinolone or an second-line injectable, but not both. Resistance is indicated in the drug profile of Table 14. The *Mtb* lineage and efficacy data are also presented.

Table 14 - Efficacy Against Resistant *Mtb*

Lineage	**Drug Profile**	**MIC (mM)**
M. tuberculosis Control	Susceptible	0.25
Atypical Beijing	XDR	0.125
Atypical Beijing	XDR	0.125
Typical Beijing	XDR	0.25
Typical Beijing	XDR	0.25
LAM	Pre-XDR	0.125
LAM	Pre-XDR	0.25
X1-Fam	Pre-XDR	0.125
X1-Fam	Pre-XDR	0.125
Beijing	MDR	
LAM 3 (F11)	RMP-mono	
S Fam (F28)	INH-mono	

In Vivo Safety and Efficacy of Benzofuran Derivative Inhibitors

Inhibitor 32 in Wild-Type Mice

To determine the in vivo safety and efficacy of representative inhibitor 32, the inhibitor was experimentally administered to *Mtb*-infected wild-type female Balb/C mice. The inhibitor was administered as a single dose of 300 mg/kg administered once daily five times per week for four weeks by oral gavage in 200 uL of canola oil. Efficacy was evaluated by determining log

reduction in *Mtb* colony forming units (CFU) and relative light units (RLU) (an index of bacterial load detected by standard ATP-Luciferase assay) after 27 day *Mtb* incubation followed by 27 day treatment as described. Efficacy was evaluated with comparison to untreated and isoniazid-treated (25 mg/kg) mice.

Bacterial CFU and RLU data in the lung and spleen for the various treatment groups is provided in Table 15 below. The inhibitor showed activity comparable to that of the current front-line drug isoniazid in both the lungs and the spleen after 4 weeks of treatment. The log reduction in *Mtb* colony forming units in the lungs of Inhibitor 32 treated mice, relative to that of the untreated controls, was 0.88, which was statistically significant ($p=0.01$). Inhibitor 32 treatment reduced the spleen burdens by 2.23 logs relative to that of the untreated control ($p<0.001$). The isoniazid control treatment gave a 1.11 log reduction in the lungs and a 2.52 log reduction in the spleen, which is consistent with previous observations. These observations were consistent with histologic observations after sacrifice.

Table 15: Mtb CFU and RLU in Inhibitor 32 treated- and control mice

Treatment	**n**	**Lung**				**Spleen**			
		CFU	SEM	RLU	SEM	CFU	SEM	RLU	SEM
Pretreatment	5/5	7.38	0.07	4.84	0.08	5.52	0.09	2.75	0.11
Inhibitor 32	5/5	5.21	0.12	2.7	0.09	2.64	0.17	1.69	0.08
Isoniazid	5/5	4.98	0.07	2.37	0.04	2.35	0.08	1.59	0.06
Untreated	5/5	6.09	0.27	3.38	0.18	4.87	0.17	2.31	0.1

There was no statistically significant difference in CFU between isoniazid and Inhibitor 32 treated mice in either the lungs or the spleen, indicating that the two drugs performed equally well. The treated mice tolerated dosing well over the four-week course of treatment, and mouse weights of all groups remained stable over the course of treatment. Experimental data and statistical analyses are provided in Table 16 below.

Table 16: Statistical comparison of treatment efficacy

Comparison	**Diff of Means**	**p**	**q**	**P**	**P<0.050**
Control vs. Isoniazid	2.523	3	17.179	<0.001	Yes

Control vs. Inhibitor 32	2.228	3	15.17	<0.001	Yes
Inhibitor 32 vs. Isoniazid	0.295	3	2.009	0.362	No

Inhibitor 32, Inhibitor 17, Inhibitor 31, and Inhibitor 47 in GKO Mice

Subsequently, the in vivo safety and efficacy of representative inhibitors, Inhibitor 32, Inhibitor 17, Inhibitor 31, and Inhibitor 47 was evaluated and compared in knockout mice engineered to lack expression of γ-interferon for rapid *in vivo* screening method for testing efficacy of inhibitors against acute infection of *M. tuberculosis*. With the exception discussed below, efficacy was evaluated after 13 day *Mtb* incubation followed by once-daily administration for nine consecutive days. As before, each treatment was administered as a single drug by oral gavage of 200 μL in canola oil. Efficacy was evaluated by determining log reduction in *Mtb* colony forming units and relative light units (RLU) in comparison to untreated and isoniazid-treated (25 mg/kg) mice.

Significant differences in efficacy and drug tolerance were observed between the four inhibitors. Treatment with 300 mg/kg dosing of Inhibitor 32 resulted in a 1.18 log CFU reduction in the Lungs relative to that of the untreated controls which was statistically significant ($p<0.001$). In the Spleen, there was a 3.64 log CFU reduction compared to the untreated controls ($p<0.001$). Treatment with 100 mg/kg Inhibitor 31 resulted in a 0.84 log CFU reduction in the lungs vs. untreated controls ($p<0.001$), and a 1.54 log CFU reduction relative to the untreated controls ($p<0.001$) in the spleen. Inhibitor 47 (300mg/kg dosing) did not show any activity in either the lungs or the spleen.

Inhibitor 17 treated mice, while initially dosed at 300 mg/kg, were dosed at 200 mg/kg beginning on day four of dosing due to apparent toxicity (one animal had a seizure and was euthanized). The remaining four animals were sacrificed on day 8 of dosing due to apparent toxicity which manifested on day 8 as seizures in two of the animals. One untreated control animal was also sacrificed on day 8 of dosing to serve as a comparator. The log CFU reduction versus the untreated control in the lungs was 0.53, and in the spleen 3.72. Because it was necessary to sacrifice these animals early, on day 8 of dosing, there was not the typical 24 hour period of drug clearance allowed prior to recovery and plating of the organ homogenates and it is

therefore possible that drug carryover could give an erroneously low CFU. These data should therefore be interpreted with caution.

The isoniazid-treated controls showed a 3.02 log CFU reduction relative to the untreated control in the lungs, and a 4.16 log CFU reduction in the spleen, which is consistent with previous results.

Luciferase assay data correlated well with CFU data in both lungs and spleen, with the log RLUs approximately 2 logs lower than the CFU, which is consistent with that seen in previous GKO experiments. The lung RLU and CFU data in particular correlated closely. Inhibitor 32-treated mice showed a log reduction in RLU of 0.68, while isoniazid-treated mice showed a log reduction in RLU of 1.01. The spleen RLU data is less reliable because the CFU burden in both treatment groups was below the standard detection limits of the RLU luciferase assay (which is approximately 4.5- 5 log CFU in this model). This would account for the lower correlation between the RLU and CFU data for the spleen.

Treatment with Inhibitor 31 resulted in a 0.84 log CFU reduction in the lungs vs. untreated controls ($p<0.001$), and a 1.54 log CFU reduction relative to the untreated controls ($p<0.001$) in the spleen. Luciferase assay data correlated well with CFU data in both lungs and spleen, with log RLUs approximately 2 logs lower than the CFU, which is consistent with that seen in previous GKO experiments.

Experimental data and statistical analyses are provided in Tables 18-18 below.

Table 17: In Vivo Efficacy Data for Representative Inhibitors

Treatment		**Lung**				**Spleen**			
	n*	CFU	SEM	RLU	SEM	CFU	SEM	RLU	SEM
Pretreatment	5/5	7.15	0.07	4.73	0.03	4.61	0.12	4.26	0.08
Untreated	1/1	7.74	N/A	5.69	0.09	6.73	N/A	4.4	0.15
Inhibitor 17	4/4	7.21	0.09	4.24	0.08	3.01	0.11	1.85	0.06
Inhibitor 32	5/5	6.99	0.14	3.88	0.1	3.01	0.16	1.81	0.08
Inhibitor 31	5/5	7.33	0.12	5.06	0.07	5.11	0.22	2.59	0.15
Inhibitor 47	5/5	8.39	0.13	6.09	0.12	6.84	0.19	4.45	0.13
Isoniazid	5/5	5.15	0.03	3.51	0.11	2.49	0.1	1.77	0.05
Control	5/5	8.17	0.08	5.69	0.09	6.65	0.05	4.4	0.15

Table 18: Statistical Comparison of Inhibitor 31 and Inhibitor 32 Treatment Efficacy

Comparison	Organ	Diff of Means	p	q	P
Control vs. Isoniazid (p = 4)	Lung	3.013	4	28.988	<0.001
	Spleen	3.644	4	24.83	<0.001
Control vs. Inhibitor 32 (p = 4)	Lung	1.174	4	11.296	<0.001
	Spleen	1.543	4	10.515	<0.001
Control vs. Inhibitor 31 (p = 4)	Lung	0.834	4	8.025	<0.001
	Spleen	2.623	4	17.874	<0.001
Inhibitor 31 vs. Isoniazid (p = 4)	Lung	2.179	4	20.963	<0.001
	Spleen	2.101	4	14.315	<0.001
Inhibitor 31 vs. Inhibitor 32 (p = 4)	Lung	0.340	4	3.271	0.137
	Spleen	0.522	4	3.558	0.095

Experimental Methods

Cloning and Overexpression of Mtb Pks13 TE Domain Construct

The TE domain constructs corresponding to the predicted TE domain in *Mtb* Pks13 gene (Rv3800c) were made by PCR from the *Mtb* H37Rv genomic DNA as the template. The amplified DNA fragments were incorporated into the pMCSG-19b vector by ligation independent cloning (LIC) to yield TEV protease cleavable N-terminal His_6-tagged TE domain constructs. The Pks13-TE-pMCSG-19b vectors were transformed into *E. coli* BL21(DE3)pLysS cells (Novagen) and the transformed cells were grown at 37 °C in LB media containing carbenicillin (100 μg/ml) and chloramphenicol (34 μg/ml) to an OD_{600} of 0.6. Expression of TE constructs was induced with 0.5 mM IPTG, and cells were harvested after 16 hours of growth at 20 °C.

The D1607N and D1644G mutants of Pks13 TE domain were constructed using the QuikChange site-directed mutagenesis kit (Stratagene). The mutations were confirmed by DNA sequencing. Mutant plasmids were transformed into *E. coli* BL21(DE3)pLysS cells, and mutant proteins were expressed by induction with 0.5 mM IPTG at 20 °C for 18 h.

Purification of Pks13 TE Domain

The harvested cells were resuspended in the lysis buffer (50 mM Tris-HCl pH 8.0, 0.5 M

NaCl, 10% (v/v) glycerol, 1 mM β-mercaptoethanol (BME) and DNase) and lysed by French press. The resulting cell extract was clarified by centrifugation (15,000 x *g*) for 1 hour at 4 °C. The cleared supernatant was loaded onto a Ni-affinity column and the His-tagged TE domain constructs were eluted with a linear gradient of 10-250 mM imidazole in 20 mM Tris-HCl, pH 8.0 and 0.5 M NaCl. The peak fractions were pooled and the His-tag was cleaved by overnight incubation with TEV protease in dialysis buffer (20 mM Tris-HCl pH 8.0, 10% (v/v) glycerol and 1 mM DTT). The TEV cleaved protein was passed through Ni-column to remove any uncleaved His-tagged protein using 20 mM Tris-HCl (pH 8.0) with 100 mM NaCl and 1 mM BME. His-tag cleaved protein eluted in the flow-through and was concentrated for loading onto a Superdex-200 gel filtration column (GE Healthcare). The TE domain constructs eluted under a single peak as a monomer (~32 kDa) from the gel filtration column and were >95% pure as observed by SDS-PAGE. The purified protein was concentrated to 20-25 mg/ml, flash-frozen and stored at -80 °C. The TE domain mutants were purified using the same protocol as for the wild-type TE domain constructs. Both the mutants and the wild-type TE domain protein constructs have the amino acids SNA from the TEV cleavage site appended to the N-terminus.

Crystallization and Soaking with Ligands

Initial screening for crystallization conditions for the soluble TE domain constructs was done by sitting drop method using 1 µl of purified protein (15-20 mg/ml) and 1 µl of crystallization buffer from the well solution. After extensive screening, crystals were obtained for only the 283 residue long construct of the TE domain starting from residue 1451 in full length Pks13 (referred to as Pks13-TE in this paper). The Pks13-TE crystals were obtained in crystallization buffer containing 0.1 M Tris-HCl, pH 8.5 and 2.0-1.8 M ammonium sulfate as precipitant. The crystals were further optimized by using polypropylene glycol P-400 as an additive at 2%-5% (v/v) in the original condition. To obtain Pks13-TE-inhibitor complex crystals, soaking of the inhibitors was done by transferring apo-Pks13-TE crystals into a drop consisting of 0.1 M Tris-HCl, pH 8.5 and 2-2.2 M ammonium sulfate with 1-2.5 mM inhibitor added from a DMSO stock keeping the final DMSO concentration at <5%, and incubated at 18 °C and 4 °C for 4-20 hours.

Crystals of the TE11451:D1607N mutant were obtained by sitting drop method at 18 °C. The crystallization drops contained an equal volume of the protein solution (15-20 mg/ml) and mother liquor (0.1 M HEPES, pH 7.5, 2%-4% (v/v) PEG 400, and 1.8-2 M ammonium sulfate), and the diffraction quality crystals were obtained within 2 weeks.

Data collection and processing

For diffraction data collection the crystals were cryo-protected using either Fomblin (Sigma) or 2.4 M malonate (Hampton Research) and flash frozen in liquid nitrogen. High resolution data was collected at a wavelength of 0.98 Å on the beamlines 19-ID and 23-ID at the Advanced Photon Source (APS) of the Argonne National Laboratory. All the data sets were processed and scaled with HKL2000. Analysis of the integrated and scaled data by Xprep indicated that Pks13-TE crystallized in $P2_12_12$ space group. Solvent content analysis indicated the presence of two molecules (V_M 2.16, V_S 43.2%) in the asymmetric unit.

Determination of Pks13-TE Atructures and Model Refinement

The structure of the TE domain was solved by molecular replacement method (MR) using *E. coli* EntF (PDB code 3TEJ), as search model. A single MR solution was obtained using Phenix AutoMR which was input into the AutoBuild wizard to generate the initial model for apo-Pks13-TE. The initial model was improved by further manual rebuilding in COOT. The final model was obtained after iterative cycles of model building and Phenix refinement with simulated annealing yielding a 1.72 Å resolution apo-Pks13-TE model with R_{cryst} of 17% and an R_{free} of 20% with good stereochemistry. The final refined apo-model has two chains, designated A and B, and 388 water molecules in the asymmetric unit.

To solve the Pks13-TE-inhibitor complex structures, as well as the D1607N mutant structure, only the protein atoms from chain A of the apo-Pks13-TE structure were used as search model in the initial rigid body refinement of the isomorphous $P2_12_12$ crystals in the Phenix Refine module. Inspection of electron density maps showed clear $|F_o-F_c|$ positive difference density for the ligands which were fit into the density using Ligandfit routine in Phenix. The ligand model and geometry restraint files were created in ELBOW BUILDER of the Phenix suite. Iterative cycles of model building and NCS-restrained maximum likelihood

refinement with simulated annealing in Phenix refine yielded high quality models for Pks13-TE-inhibitor complexes. Some of the residues in Pks13-TE structures at the flexible N- and C-termini, and the loops of the lid domain could not be built into the model due to the missing electron density, and some of the residues which showed ambiguous side chain electron density were modeled as alanines. In all of the structures >98% of residues are placed in the favored region of the Ramachandran plot as determined by MolProbity validation tool in Phenix.

Enzyme Assay

Activity of Pks13-TE was assessed using 4-methylumbelliferyl heptanoate (4-MUH, Sigma) as a fluorogenic substrate in a 96-well plate format. To make initial velocity measurements, Pks13-TE (1 μM) in 0.1 M Tris-HCl, pH 7 buffer was incubated with different concentrations of 4-MUH (2-150 μM in DMSO) in a 100 μl reaction volume, and the fluorescence of the hydrolyzed product 4-methylumbelliferone was read (excitation at 355 nm and emission at 460 nm) using PolarStar Omega plate reader (BMG Labtech) at 5-10 min intervals over 60-70 min. The reaction rate was observed to be linear in the measured range. 4-MUH in buffer alone was included as a control to quantify its background hydrolysis. Data points were plotted as an average of triplicates and each experiment was repeated 2-3 times independently. The initial velocity data was curve fit to Michaelis-Menten equation by nonlinear regression using Prism software (Graphpad) to determine the kinetic parameters K_m and V_{max}. The assay and data analysis for Pks13-TE mutants was done the same way as that for the wild-type protein with the 4-MUH concentration varying from 2 to 300 μM.

IC_{50} Determination

To determine the potency of the test compound and its analogs against wt Pks13-TE, the compounds were tested at concentrations ranging from 0.012 to 20 μM in a 96-well plate format. The reaction mix contained 0.1 μM Pks13-TE in 0.1 M Tris-HCl, pH 7 buffer with 1 μl of each dilution of the compound or DMSO in a total volume of 99 μl. The reaction was initiated by addition of 1 μl of 2 mM 4-MUH in DMSO (20 μM final concentration) to the reaction mix. Initial velocity data was obtained by monitoring increase in the fluorescence due to hydrolysis of the substrate using PolarStar Omega plate reader at 10 min intervals over 60 min. The data

points were collected in triplicate and the averaged value was used to generate concentration-response plots for the test compound and its analogs. The IC_{50} value for each compound was obtained by nonlinear regression curve fitting of a four-parameter variable slope equation to the dose-response data using Prism software. The IC_{50} values of the test compound for Pks13-TE mutants were determined in the same way as that for wt Pks13-TE, however, the testing concentration of the test compound ranged from 0.04 to 40 μM and the substrate 4-MUH was used at a final concentration of 20 μM in the reaction mixture.

Whole Cell and Cytotoxicity Testing

Whole cell testing for determining MIC was done using Alamarblue assay in 96-well plates. *Mtb* mc^2-7000 strain cells were grown in 7H9 media supplemented with OADC (Middlebrook), 0.05% Tyloxapol (Sigma), and 25 mg/ml pantothenate to an OD_{600} of 1–2. The cells were then diluted into testing media (7H9 media with 0.2% dextrose, 0.085% NaCl, 0.05% Tyloxapol, and 25 mg/ml pantothenate) to an OD_{600} of 0.01 and dispensed into testing plates at 200 μl per well. Then the compounds were added as a 2-fold serial dilution in DMSO (2% DMSO final in each well). The test plates also had a DMSO only control and a Rifampicin control. The plates were incubated with shaking at 37 °C for 6 days and then stained with resazurin (Sigma) for an additional 2 days at 37 °C. After staining the fluorescence of reduced resazurin was read (λ_{Ex} = 544 nm, λ_{Em} = 590 nm) using PolarStar Omega plate reader. The fluorescence data were plotted as percent growth inhibition against the compound concentration and curve fitting was done by nonlinear regression using Prism software. Minimum inhibitory concentration (MIC) values were determined from the fitted curves.

Compounds were tested for toxicity by the Human Dermal Fibroblast (HDF) cytotoxicity assay. HDF cells were purchased from ATCC (Manassas, VA). The cells were cultured in DMEM (Lonza) media supplemented with 10% fetal bovine serum (Lonza) and penicillin/streptomycin (Lonza). For setting the cytotoxicity assay, compound stocks were serially diluted in phosphate buffered saline (PBS) plus 10% DMSO. On the day of assay, HDF cells were trypsinized, counted and resuspended at a concentration of 64,000 cells/ml in the media. Cells were plated, overlaid with the compound serial dilutions and incubated at 37 °C. After 48 h, resazurin dye was added and the assay plates were cultured for another 24 h. The

next day the absorbance of the resazurin was measured on a microplate reader (BMG Labtech) to assess cell death. Cytotoxicity was determined as a percent of dead cells versus living cells.

In Vivo Efficacy and Safety

6-8 week old Balb/C female mice from Charles River were rested at least one week prior to Mtb infection with ~50-100 bacilli/mouse (Erdman lux strain lot # 11/20/08) by Low Dose Aerosol administration via Glas-Col Inhalation Exposure System. Whole lungs and spleens were extracted and homogenized in PBS. CFU was determined by counting after plating homogenates on 7H-11 agar plates and incubating in a 37° C dry-air incubator for ~3 weeks. Therapy, administered via oral gavage, was started on day 27 post-infection and continued for 4 weeks. Drugs were administered daily, for 5 days a week, by oral gavage in a volume of 200 µl/animal in canola oil. After one month of treatment; 5- 6 mice from each group (untreated and drug treated mice) were sacrificed and bacterial loads were determined. Plating of lung and spleen homogenate was conducted as described above.

* * *

While numerous changes may be made by those skilled in the art, such changes are encompassed within the spirit of this invention as illustrated, in part, by the appended claims.

CLAIMS

1. A composition comprising at least one benzofuran derivative having the following formula:

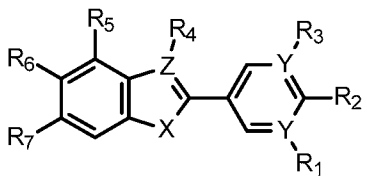

,

wherein:

X is O or NH;

each Y group is independently selected from C and N;

Z is C or N;

R_1, R_2 and R_3 are independently selected from hydrogen, methoxy, hydroxyl, fluoro, nitrile, and carboxamide moieties;

R_4 is selected from the group consisting of CH_2OH, COOEt, COOH, CONHMe, CONHEt, and amides of cyclic and acyclic secondary or tertiary amines;

R_5 is an alkyl, cyclic alkyl, or heterocyclic alkyl group, optionally substituted with substituents selected from hydroxyl, alkoxy, halogen, amine, alkylamine, hydroxyalkylamine, dialkylamine, dialkylaminealkyl, carboxy, carboxamide, acylamine, sulfoxide, sulfone, aryl, heteroaryl, and heterocyclic groups;

R_6 is selected from H, OMe, and OH; and

R_7 is selected from H, NO_2, NH_2, and NHAc.

2. The composition of claim 1, wherein the at least one benzofuran derivative is not:

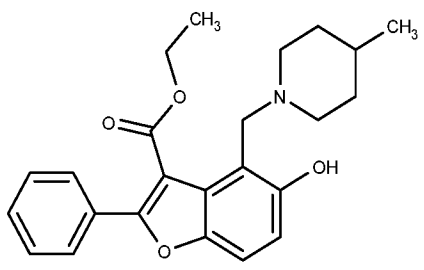

.

3. The composition of any of the preceding claims, wherein the R_2 substituent of the at least one benzofuran derivative is a hydroxyl moiety.

4. The composition of any of the preceding claims, wherein the R_4 substituent of the at least one benzofuran derivative is a CONHMe moiety.

5. The composition of any of the preceding claims, wherein the at least one benzofuran derivative has a half-maximal inhibitory concentration against wild-type Pks13 thioesterase of 0.25 μM or less.

6. The composition of any of the preceding claims, wherein the at least one benzofuran derivative has a minimum inhibitory concentration against *Mycobacterium tuberculosis* bacilli of 2 μM or less.

7. The composition of any of the preceding claims, wherein the at least one benzofuran derivative is selected from the group consisting of Inhibitor 31 and Inhibitor 32.

8. A method of inhibiting a bacterium in a patient comprising administering to the patient, in an amount effective to inhibit the bacterium, a composition of any of the preceding claims.

9. The method of claim 8, wherein the bacterium is a Mycobacterium.

10. The method of claim 8 or claim 9, wherein the Mycobacterium is *Mycobacterium tuberculosis*.

11. The method of any of claims 8-10, further comprising administering to the patient at least one additional antibiotic drug.

12. The method of claim 11, wherein the at least one additional antibiotic drug is selected from the group consisting of with one or more drugs selected from the group consisting of isoniazid, rifampicin, pyrazinamide, ethambutol, rifapentine, rifabutin. streptomycin, kanamycin, and amikacin, capreomycin, viomycin, ciprofloxacin, levofloxacin, moxifloxacin, ofloxacin, gatifloxacin, *para*-aminosalicylic acid, cycloserine, terizidone, ethionamide,

prothionamide, thioacetazone, linezolid, clofazimine, amoxicillin, clavulanate, imipenem, cilastatin, and clarithromycin.

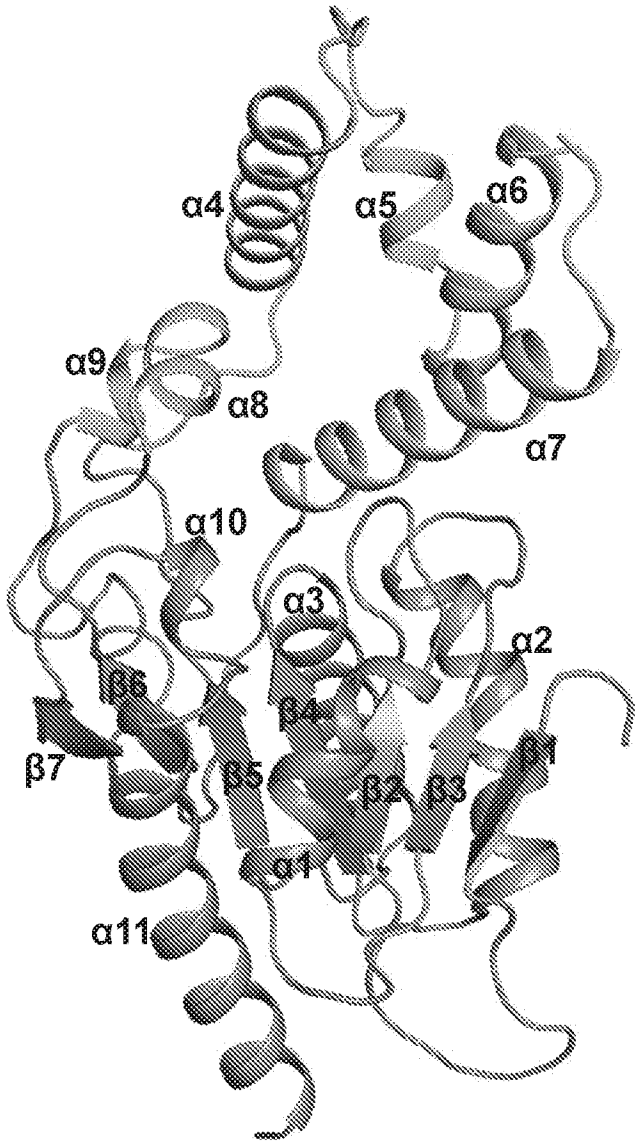

FIG. 1

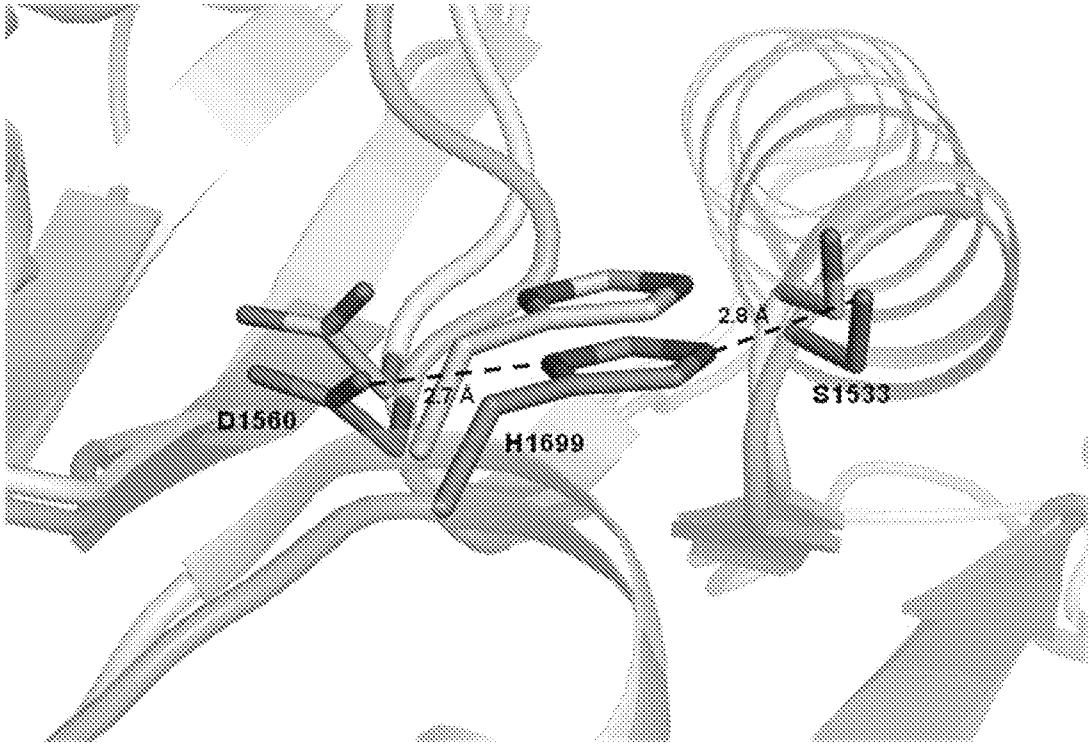

FIG. 2

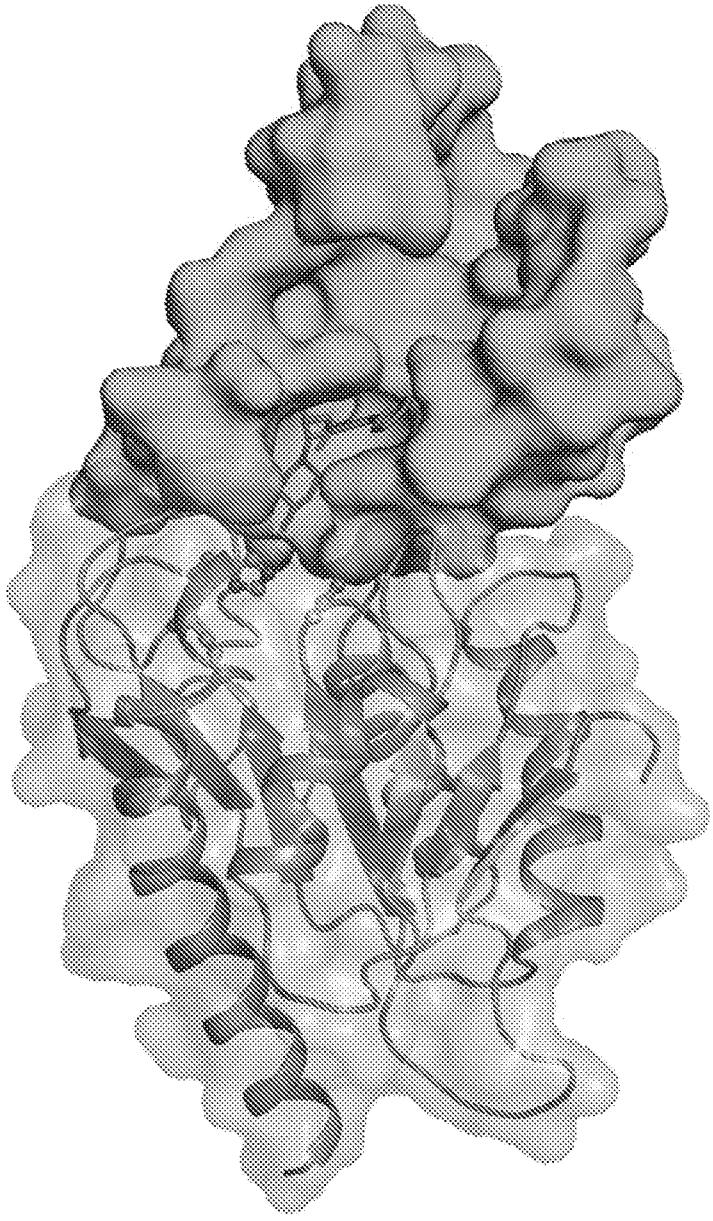

FIG. 3

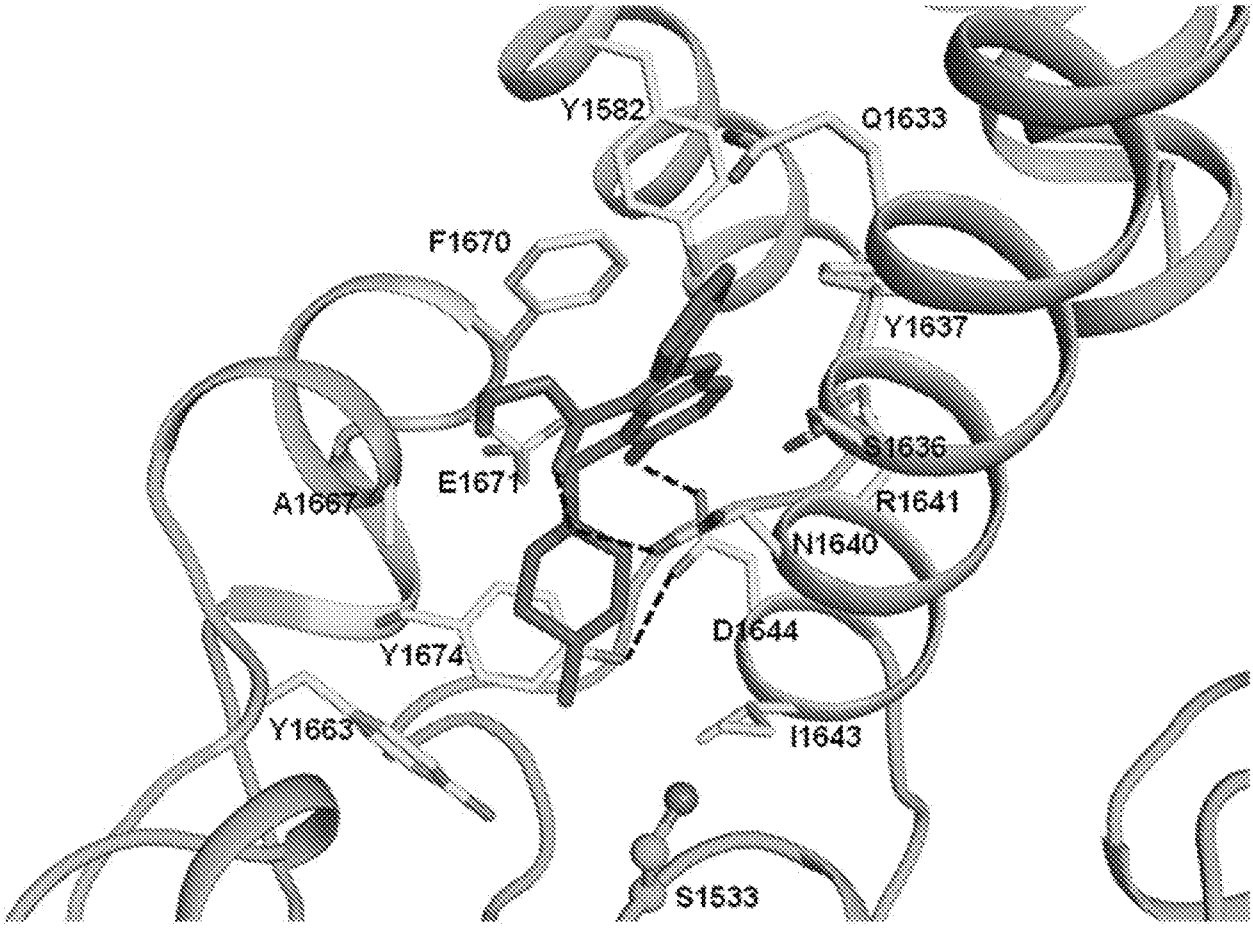
Y1582
Q1633
F1670
Y1637
S1636
E1671
A1667
R1641
N1640
D1644
Y1674
Y1663
I1643
S1533

FIG. 4

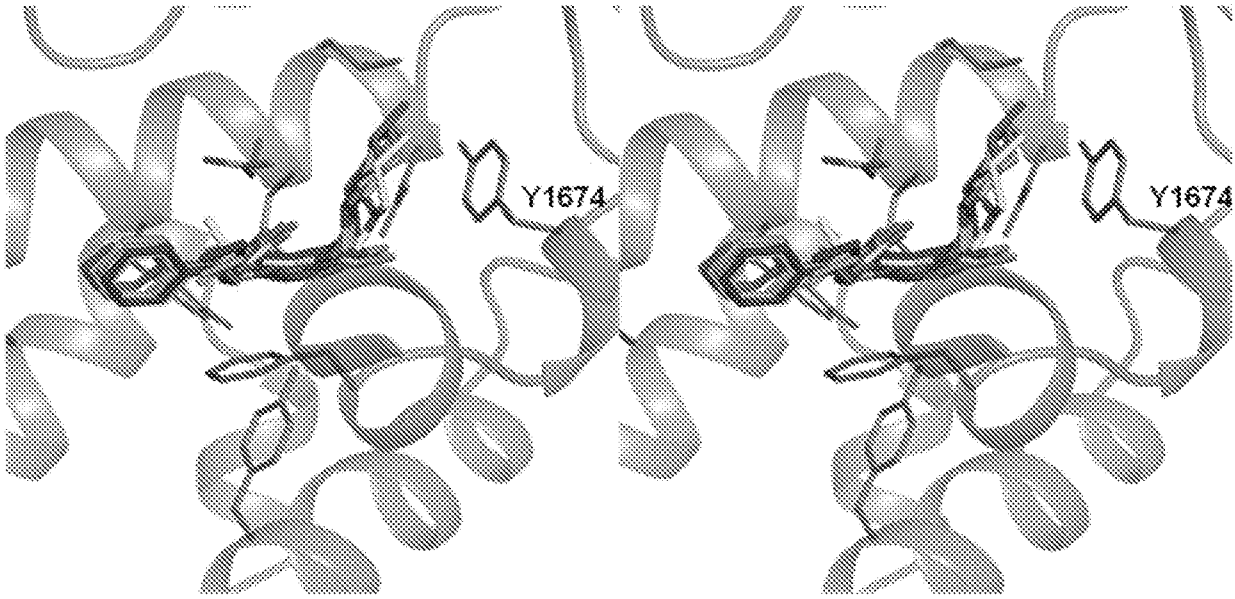

FIG. 5

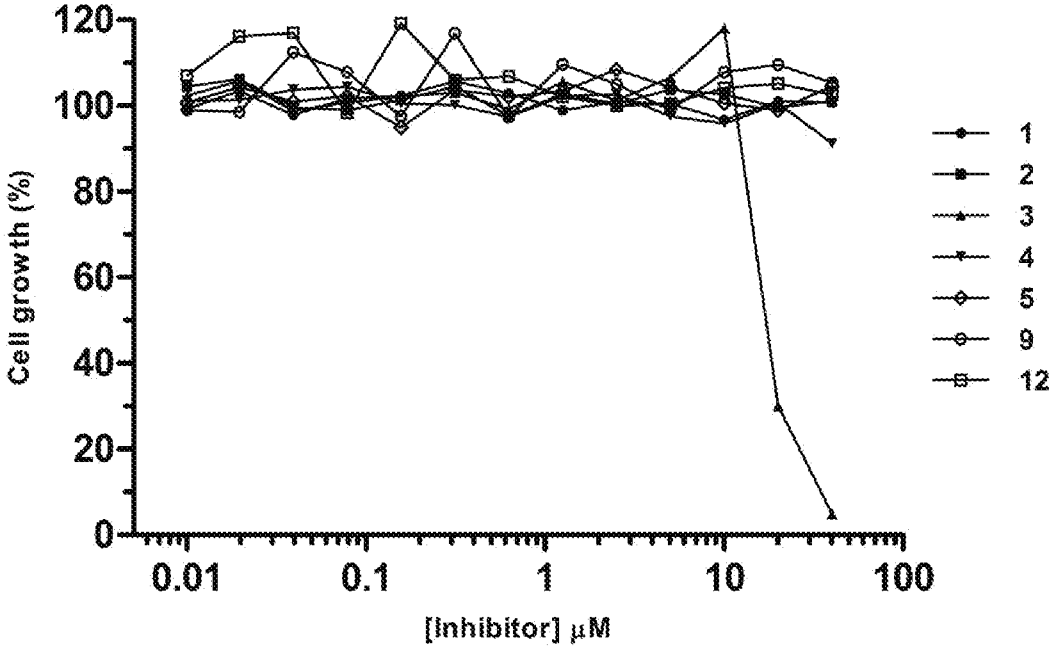
120
100
80
60
40
20
0
Cell growth (%)
0.01
0.1
1
10
100
[Inhibitor] μM
1
2
3
4
5
9
12

FIG. 6

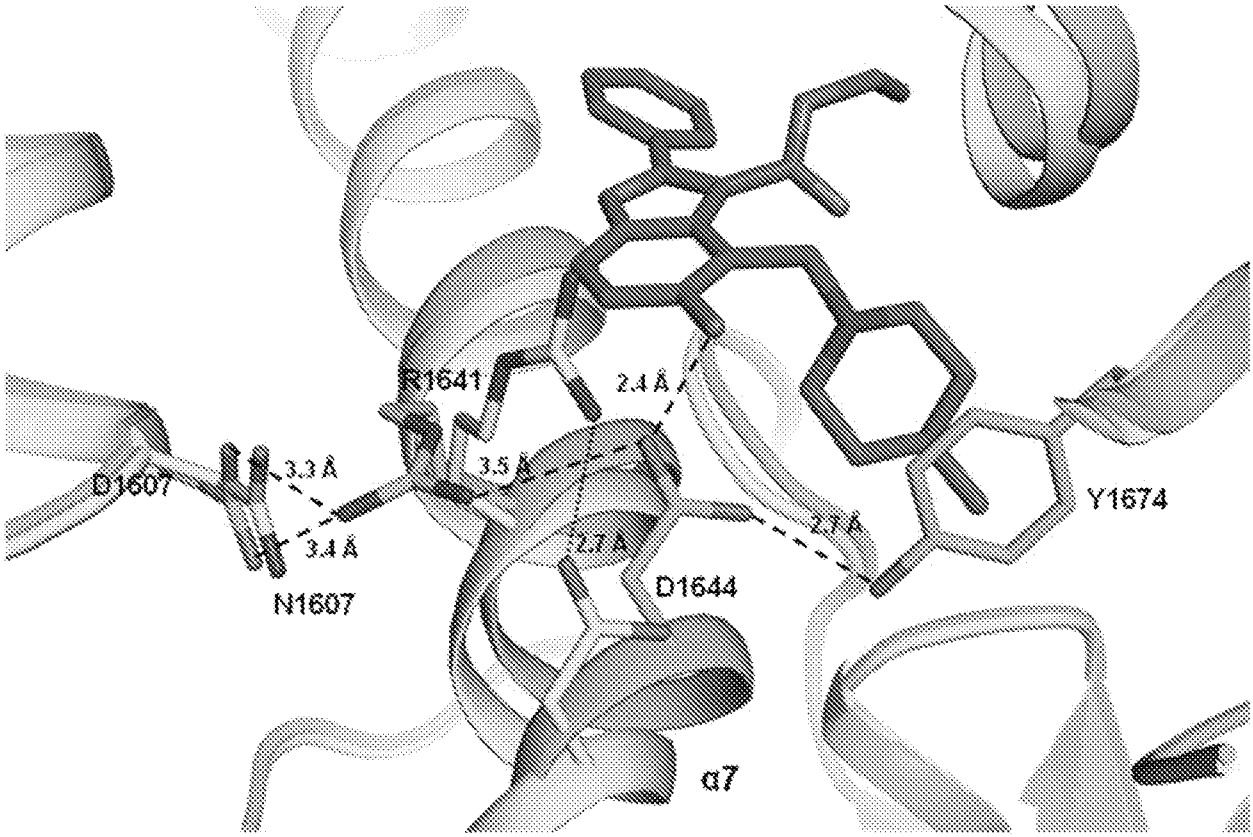

FIG. 7

INTERNATIONAL SEARCH REPORT

International application No.
PCT/US16/28867

A. CLASSIFICATION OF SUBJECT MATTER
IPC(8) - A61P 31/06; A61K 31/4164, 31/505 (2016.01)
CPC - A61K 31/4015, 31/381, 31/19
According to International Patent Classification (IPC) or to both national classification and IPC

B. FIELDS SEARCHED

Minimum documentation searched (classification system followed by classification symbols)
IPC(8): A61P 31/06; A61K 31/4164, 31/505 (2016.01)
CPC: A61K 31/4015, 31/381, 31/19

Documentation searched other than minimum documentation to the extent that such documents are included in the fields searched

Electronic data base consulted during the international search (name of data base and, where practicable, search terms used)
PatSeer (US, EP, WO, JP, DE, GB, CN, FR, KR, ES, AU, IN, CA, Other Countries (INPADOC), RU, AT, CH, TH, BR, PH); EBSCO; Google/Google Scholar, IP.com: benzofuran, antimycobacterial, Pks13, enzyme, tuberculosis, mycobacterium, isoniazid

C. DOCUMENTS CONSIDERED TO BE RELEVANT

Category*	Citation of document, with indication, where appropriate, of the relevant passages	Relevant to claim No.
X	US 2006/0194851 A1 (OISHI, Y et al.) 31 August 2006; paragraphs [0007], [0015], [0017], [0021]-[0025], [0027]-[0028], [0222], [0251], [0271]	1-2, 3/1-2
A	US 2014/0179735 A1 (ZHANG, ZY et al.) 26 June 2014; entire document	1-2, 3/1-2
A	US 2010/0113477 A1 (FREUNDLICH, JS et al.) 06 May 2010; entire document	1-2, 3/1-2

☐ Further documents are listed in the continuation of Box C. ☐ See patent family annex.

* Special categories of cited documents:
"A" document defining the general state of the art which is not considered to be of particular relevance
"E" earlier application or patent but published on or after the international filing date
"L" document which may throw doubts on priority claim(s) or which is cited to establish the publication date of another citation or other special reason (as specified)
"O" document referring to an oral disclosure, use, exhibition or other means
"P" document published prior to the international filing date but later than the priority date claimed
"T" later document published after the international filing date or priority date and not in conflict with the application but cited to understand the principle or theory underlying the invention
"X" document of particular relevance; the claimed invention cannot be considered novel or cannot be considered to involve an inventive step when the document is taken alone
"Y" document of particular relevance; the claimed invention cannot be considered to involve an inventive step when the document is combined with one or more other such documents, such combination being obvious to a person skilled in the art
"&" document member of the same patent family

Date of the actual completion of the international search	Date of mailing of the international search report
08 June 2016 (08.06.2016)	12 JUL 2016

Name and mailing address of the ISA/	Authorized officer
Mail Stop PCT, Attn: ISA/US, Commissioner for Patents P.O. Box 1450, Alexandria, Virginia 22313-1450 Facsimile No. 571-273-8300	Shane Thomas PCT Helpdesk: 571-272-4300 PCT OSP: 571-272-7774

Form PCT/ISA/210 (second sheet) (January 2015)

INTERNATIONAL SEARCH REPORT

International application No.
PCT/US16/28867

Box No. II Observations where certain claims were found unsearchable (Continuation of item 2 of first sheet)

This international search report has not been established in respect of certain claims under Article 17(2)(a) for the following reasons:

1. ☐ Claims Nos.:
because they relate to subject matter not required to be searched by this Authority, namely:

2. ☐ Claims Nos.:
because they relate to parts of the international application that do not comply with the prescribed requirements to such an extent that no meaningful international search can be carried out, specifically:

3. ☒ Claims Nos.: 4-12
because they are dependent claims and are not drafted in accordance with the second and third sentences of Rule 6.4(a).

Box No. III Observations where unity of invention is lacking (Continuation of item 3 of first sheet)

This International Searching Authority found multiple inventions in this international application, as follows:

1. ☐ As all required additional search fees were timely paid by the applicant, this international search report covers all searchable claims.

2. ☐ As all searchable claims could be searched without effort justifying additional fees, this Authority did not invite payment of additional fees.

3. ☐ As only some of the required additional search fees were timely paid by the applicant, this international search report covers only those claims for which fees were paid, specifically claims Nos.:

4. ☐ No required additional search fees were timely paid by the applicant. Consequently, this international search report is restricted to the invention first mentioned in the claims; it is covered by claims Nos.:

Remark on Protest

☐ The additional search fees were accompanied by the applicant's protest and, where applicable, the payment of a protest fee.

☐ The additional search fees were accompanied by the applicant's protest but the applicable protest fee was not paid within the time limit specified in the invitation.

☐ No protest accompanied the payment of additional search fees.